Thesis for the Degree of Master of Science

Anti-diabetic and anti-Alzheimer's disease activities of oligonol

By

Himanshu Kumar Bhakta

Department of Food and Life Science

The Graduate School

Pukyong National University

August 2016

Anti-diabetic and anti-Alzheimer's disease activities of oligonol

(Oligonol 의 항당뇨 및 항 알츠하이머 활성)

Advisor: Prof. Jae Sue Choi

By

Himanshu Kumar Bhakta

A thesis submitted in partial fulfillment of the requirements for the degree of Master of Science

Department of Food and Life Science, The Graduate School

Pukyong National University

August 2016

Anti-diabetic and anti-Alzheimer's disease activities of oligonol

A dissertation

By

Himanshu Kumar Bhakta

Approved by:

_____

_____ _____

TABLE OF CONTENTS

LIST OF FIGURES

LIST OF TABLE

Anti-diabetic and anti-Alzheimer's disease activities of oligonol

Himanshu Kumar Bhakta

Department of Food and Life Science, The Graduate School,

Pukyong National University

ABSTRACT

Oligonol is a low-molecular-weight form of polyphenol that is derived from lychee fruit extract containing catechin-type monomers and proanthocyanidin oligomers. Recently, oligonol has emerged as a rich source of naturally occurring therapeutic agent, is predicted to indicate favorable effects on numerous chronic diseases, including diabetics mellitus, oxidative stress, inflammation, obesity, and cancer. The detailed mechanisms by which oligonol may act as an anti-diabetic, moreover, anti-Alzheimer's molecule haven't been determined. In this study, we investigate the anti-diabetic activities of oligonol *via* α-glucosidase and human recombinant protein tyrosine phosphatase 1B (PTP1B) assays and find out the possible mechanism of oligonol in insulin resistance HepG2 cells. This study additionally investigates the binding affinity of the constituents of oligonol on PTP1B, and *t*-BHP induced hepatoprotective effects by scavenging

peroxynitrite as well as scavenging of total and intracellular ROS generation. Moreover, investigates anti-Alzheimer's disease activities, by evaluating the ability of this compound to inhibit acetylcholinesterase (AChE), butyrylcholinesterase (BChE), and β-site amyloid precursor protein (APP) cleaving enzyme 1 (BACE1). Oligonol exhibited potent concentration-dependent anti-diabetic activities by inhibiting α-glucosidase and PTP1B with IC_{50} values of 23.14 ± 0.91 µg/mL and 1.02 ± 0.04 µg/mL, respectively. Moreover, a kinetics study revealed that oligonol inhibited α-glucosidase (K_i=22.36) and PTP1B (K_i=8.51) with characteristics typical of a mixed inhibitor. According to the cellular study, oligonol increased the insulin-provoked glucose uptake and decreased the expression of PTP1B in insulin-resistant HepG2 cells in a dose-dependent manner compared to the normal and insulin resistance group. The binding mode was determined using state-of-the-art of covalent docking and scoring methodology, which gave added support to the above results of PTP1B inhibition. The obtained data clearly demonstrated that the constituents of oligonol possess high inhibitory activity against PTP1B by bind with specific interacting residues (SER80), which shared among all of the oligonol constituents except procyanidin A1, and A2, involved in PTP1B inhibition. Further, oligonol activates the IRS-1 by decreasing the phosphorylation of IRS-1 (Ser 307) and increased the phosphorylation of Akt, PI3K, and ERK 1 significantly, as well as suppressed proinflammatory nuclear factor-kappa B (NF-κB) p65 and inhibit the caspase-3 activation significantly in insulin-resistant HepG2 cells compared to the control group. In addition, protective effects of oligonol against tertbutyl hydroperoxide (t-BHP) induced oxidative stress in HepG2 cells was determined, that showed significant hepatoprotective activity by decreasing intracellular and or total ROS (IC_{50}= 2.30 ± 0.32 µg/mL) generation dose-dependently. Oligonol also displayed potent concentration-

dependent inhibitory activity against AChE and BChE with IC_{50} values of 4.34 ± 0.06 μg/mL and 2.07 ± 0.53 μg/mL, respectively. However, oligonol exhibited only marginal concentration-dependent BACE1 inhibitory activity with an IC_{50} value 130.45 ± 1.49 μg/mL. A kinetic's study revealed mixed-type inhibition against AChE (K_i=4.65) and BACE1 (K_i=58.80), but noncompetitive-type inhibition against BChE (K_i=9.80). Furthermore, oligonol exhibited the dose-dependent scavenging activity of $ONOO^-$ with IC_{50} values of 17.98 ± 0.76 μg/mL, and inhibitory activity of peroxynitrite ($ONOO^-$)-mediated protein tyrosine nitration. Therefore, the results of the present study clearly demonstrate the promising antidiabetic, hepatoprotective, as well as anti-AD potential of oligonol.

I. Introduction

Diabetes mellitus (DM), which is a chronic and widespread metabolic disease, characterized as a consequence of genetically-based predisposition and dietary indiscretion, with high prevalence and mortality rates in all over the world (Wang et al. 2013). The major biochemical alterations in diabetes are hyperglycemia and dyslipidemia, caused by the combination of resistance to insulin action, inadequate insulin secretion, and excessive glucagon secretion (Srikanthan et al. 2004), that responsible for various metabolic complications. The complications of DM are directly or indirectly correlated with different organ diseases, including, liver disease, apoptosis of pancreatic β-cell, chronic nephritis, and diabetic cardiomyopathy (Younossi et al. 2004; Chang-Chen et al. 2008). Type 2 diabetes mellitus (T2DM) is among the most common metabolic disorders that are characterized by various distinct defects, insulin resistance is one of them, which decrease in the ability of insulin to stimulate glucose regulation and inhibit hepatic glucose production as well inhibit the insulin signaling pathway. Moreover, relative insulin deficiency, ensuing from an inability of the pancreatic β cells to compensate for this insulin resistance by increases in insulin secretion. Recently, insulin resistance has seemed to be the core of the pathophysiology of

T2DM and other's metabolic syndrome (Taylor 2012; Mukherjee et al. 2013; Weiss et al. 2013). Insulin resistance may be a defect of post-receptor signaling of the insulin receptor, characterized by inadequate regulation of nutrient metabolism and glucose uptake, in varied tissues and organs, particularly liver (Cornier et al. 2008). The systemic regulation of glucose metabolism by insulin was discovered in 1992 (Banting et al. 1992). Currently, insulin-sensitizing medicines are unit restricted and identification of insulin stimulatory drug candidate is a big challenge (Ye 2011), that is not only a powerful indicator of disease progression but also a therapeutic target. In general, insulin signaling occurs through the PI3K/AKT and Ras/MAPK pathways that facilitate the actions of insulin on metabolism and growth-promotion, respectively (Groop et al. 2005). More specifically, insulin activates glycogen synthase to increase glycogen production in muscles and the liver, by inactivating glycogen synthase kinase-3 via the PI3K/AKT pathway (Cross et al. 1995). Insulin receptor (IR) a member of the family of tyrosine kinase receptors, which activates the PI3K/AKT signaling cascade by formed a bond with insulin. Following conjugation, a conformational modification to the IR ends up in its autophosphorylation that attracts and phosphorylates multiple tyrosine residues on numerous docking proteins, as well

insulin receptor substrates (IRS) 1 and 2 (White 2003). IRS1/2 binds and activates a family of signal transducing enzymes known as phosphatidylinositol -4,5-bisphosphate 3-kinases (PI3K), that is responsible for the phosphorylation of the membrane-bound lipoprotein phosphoinositide (4, 5)-P2 (PIP2) to PIP3 (Vanhaesebroeck et al. 1997). PIP3 may be a key molecule during this cascade because it binds and recruits both AKT and its activator phosphoinositide-dependent kinase-1 to the plasma membrane (Franke et al. 1997). The binding of inactive AKT to PIP3 causes a conformational modification in AKT that exposes its active loop, leading to its phosphorylation by phosphoinositide-dependent kinase-1 (PDPK1) at an isoform-specific threonine (Thr-308 for AKT1) (Alessi et al. 1996). PDPK1 phosphorylation stabilizes the activation loop at Thr-308, facilitating the second phosphorylation of AKT on the C-terminal (Sarbassov et al. 2005). This additional phosphorylation event potentiates AKT activity results in its full activation (Alessi et al. 1996). Phosphorylated Akt signaling cascades also have a critical role in cell survival and apoptosis regulation, while Akt promotes cell survival by inhibiting programmed cell death by phosphorylating and inactivating certain members of caspase family, especially caspase-3 (Franke et al. 2003). On the other hand, extracellular receptor-activated kinase (ERK) is

activated *via* the IR-SHC-RAF-MEK1-ERK signal transduction pathway (Saltiel and Pessin 2002; Avruch 1998). Moreover, PTP1B, which is localized within the cytoplasmatic face membrane of the endoplasmic reticulum, is wide expressed in insulin-sensitive tissues, like liver, muscle and fatty tissues (Tonks 2003). PTP1B can bind and dephosphorylate tyrosine residues of activated IR as well as IRS, resulting in impaired insulin signaling and glucose uptake (Kenner et al. 1996; Byon et al. 1998). Molecular biology researchers have proven that PTP1B overexpression inhibits phosphorylation of IR and IRS-1 that causes insulin resistance. Inhibition of PTP1B in liver, muscle, and fat tissues enhances insulin sensitivity (Klaman et al. 2000; Zabolotny et al. 2004). Thus, PTP1B has been considered as a promising insulin-sensitive drug target for the prevention and the treatment of T2DM (Zabolotny et al. 2004). Although the significance of PTP1B in regulating insulin signaling has been widely reported, the role of PTP1B as a modulator of caspase-mediated cell death was solely reported during a few papers. It was reported that PTP1B deficiency protected hepatocyte cells (Gonzalez-Rodriguez et al. 2007). Substantial epidemiological evidence shows an increased risk of developing Alzheimer's disease (AD) in patients with diabetes (Piaceri et al. 2013; Yang and Song 2013). There are several physiological factors

that are associated with both T2DM and AD, including higher cholesterol, dis-metabolism, degeneration, amyloid β (Aβ) deposition (Ristow 2004), tau protein phosphorylation, glycogen synthesis kinase 3 (Doble and Woodgett 2003), inflammation, cardiovascular disease, oxidative stress, (Haan 2006), and apoptosis (Lin 2008). Furthermore, BChE and AChE-related proteins were found to be common to both AD and diabetes; they may play an etiological role by influencing insulin resistance and lipid metabolism (Sridhar et al. 2006). Rao et al. (2007) suggest that an elevation in plasma and tissue (pancreas and brain) levels of the endogenous protein BChE provides a typical link between the two diseases and opens new pathways for potential treatment. Recent findings conjointly showed that there are close connections between the pathology ascertained within the brains of AD and DM patients (Luo et al. 2016). DM is caused by insulin resistance and a relative lack of active insulin. AD is characterized by the deposition of (Aβ) peptide fibrils. Insulin can also form amyloid fibrils. In the brain, insulin plays a pivotal role in neuronal functions by differentiation, regulating energy metabolism, growth, and survival via insulin signaling (Lacroix et al. 2008). Thus, perverse insulin signaling causes an alteration in the signaling pathway, leading to an AD-like pattern of reduced

cerebral glucose metabolic rate in the brain (Kuwabara et al. 2011). According to the molecular studies, are shown that insulin and Aβ affect each other's degradation, production, and function (Takeda et al. 2011). Insulin stimulates the activity of γ-secretase in Aβ secretion, results in an increase the level of extracellular Aβ (Phiel et al. 2003). Furthermore, Aβ degradation is inhibited by blocking the activity of the insulin-degrading enzyme in neuronal and microglial cells (Qiu et al. 2006). The pathogenesis of AD, associated with insulin signal transduction that regulates the activity of hyperphosphorylated tau in the formation of AD neurofibrillary tangles *via* the glycogen synthase kinase (Gasparini et al. 2002; Takeda et al. 2011). On the other hand, Aβ competes with insulin for binding at the insulin receptor and inhibits the effect of insulin on the secretion of the Aβ precursor protein. In spite of the fact there some of the research had been shown that Aβ may induce insulin resistance, by reducing the signal transduction activity in the insulin receptor, the insulin/Aβ cross regulation remains to be fully clarified (Ling et al. 2002; Zhao et al. 2008).

Moreover, oxidative stress also associated with diabetes as well as in Alzheimer's disease (Reddy et al. 2009). Increased lipid peroxidation and reactive oxygen species (ROS) activate stress-sensitive intracellular signaling pathways

such as the transcription of NF-κB, which plays a central role in DM and AD. Additionally, there is a well-known connection between the main pathological features of AD with glucose metabolic intermediates, insulin receptors, and insulin transporters, all in the same context of oxidative stress, arises due to the intracellular imbalance in the production of reactive oxygen/reactive nitrogen species and cellular antioxidant defense mechanisms (Rosales-Corral et al. 2015). Tert-butyl hydroperoxide (*t*-BHP) is an organic peroxide, triggers the generation of harmful free radical intermediates, such as peroxyl and alkoxyl radicals, which directly cross the cell membranes and lead to the production of highly reactive hydroxyl radicals, thereby leading to cell death (Grunberger et al. 1988). Recently, identifying the natural agents that can show protective effects against *t*-BHP induced cytotoxicity is a great deal. In these studies, HepG2 was used for the screening of hepatoprotective agents against *t*-BHPand induced cytotoxicity, because this cell line is known to retain many of the relevant cellular functions. Thus, nitrotyrosine is now generally considered a collective index of reactive nitrogen species, rather than a specific indicator of the peroxynitrite ($ONOO^-$) formation. The $ONOO^-$, formed by the reaction between nitric oxide and superoxide, is a powerful oxidant capable of oxidizing several lipoproteins and of

nitrating tyrosine residues in many proteins, which have been shown to have direct and deleterious consequences in diabetes and Alzheimer's disease (Ceriello et al. 2001; Reddy et al. 2009). Recently, efforts have shifted towards identifying effective therapeutic agents for metabolic and neurodegenerative disorders such as DM and AD from natural sources, due to the toxic and undesirable side effects that are associated with synthetic drugs. Functional foods and/or dietary ingredients with health benefits attract a great deal of attention due to the absence of adverse effects, abundant production, and application of various commercial products (Jones and Varady 2008). In particular, polyphenol-rich foods, such as wine, tea, coffee, and chocolate, have received considerable attention as dietary sources of antioxidants that are valuable in human health (Nakayama et al. 1993; Hsieh and Wu 1999; Pal et al. 2001).

Lychee (*Litchi chinensis,* Sapindaceae) is rich in polyphenol, a subtropical fruit, is widely cultivated in Africa, South-East Asia, such as Bangladesh, India, China, Taiwan, and Japan etc (Wang et al. 2011; Jiang et al. 2013). Oligonol is a novel product derived from the oligomerization of polyphenols, typically proanthocyanidins from a variety of fruits, including lychees, grapes, apples and persimmons. Brat et al. (2006) reported that lychee polyphenol content per edible

part is second only to strawberries. A particular feature of lychee polyphenol is a phenolic product containing catechin-type monomers and oligomers of proanthocyanidins. There is evidence that oligonol can exert some biological effects *in vitro* and *in vivo*, including anti-cancer (Jo et al. 2007), antioxidant, and anti-inflammatory effects (Kundu et al. 2008), beneficial activity in nitric oxide bioavailability (Zhang et al. 2010), and a regulatory effect on lipid metabolism (Sakurai et at. 2008; Ogasawara et al. 2009). Although, oligonol has anti-DM and anti-AD properties, until now, the mechanism of action, as well as the specific binding affinity and enzymatic inhibitory activities against DM and AD, remains unknown. Therefore, the objective of the present work is to evaluate inhibitory effects and a possible mechanism of oligonol against DM, preventive effects against oxidative stress, and anti-Alzheimer activities by using in vitro enzyme assays with kinetics' analysis as well as an insulin resistance HepG2 cells model.

II. Materials and methods

1. Materials

1.1. Plant materials

Oligonol (>95% purity) provided by the Amino Up Chemical Co., Ltd. (Sapporo, Japan), was produced from lychee fruit (*Litchi chinensis* Sonn.) extract and green tea (*Camellia sinensis*) extract using a patented technology process (international patent WO 2004/103988 Al) (Nonaka et al. 2004). The composition of oligonol is shown in Table 1. Briefly, dried lychee fruits, are extracted with 50% (v/v) ethanol. The filtrate is evaporated and passed through a DIAION HP-20 column and eluted with ethanol. The eluate is evaporated to dryness yielding a dark brown powder which contains a mixture of proanthocyanidins. The lychee extract is mixed with green tea extract, which provides an enriched source of monomeric procyanidins, and citric acid in water. The reaction mixture is heated at 60^0C for 16 hours, filtered through a DIAION HP-20 column, washed with water and eluted with 40% (v/v) ethanol. Evaporation of the eluate yields a reddish-brown powder containing the monomeric and oligomeric proanthocyanidin mixture, oligonol (Fujii et al. 2008; Kitadate et al. 2014).

Lychee fruit extract and green tea extract for the production process are provided by Guilin Layn Natural Ingredients Corp. (Guilin, China).

Fig. 1. Lychee (*Litchi chinensis*).

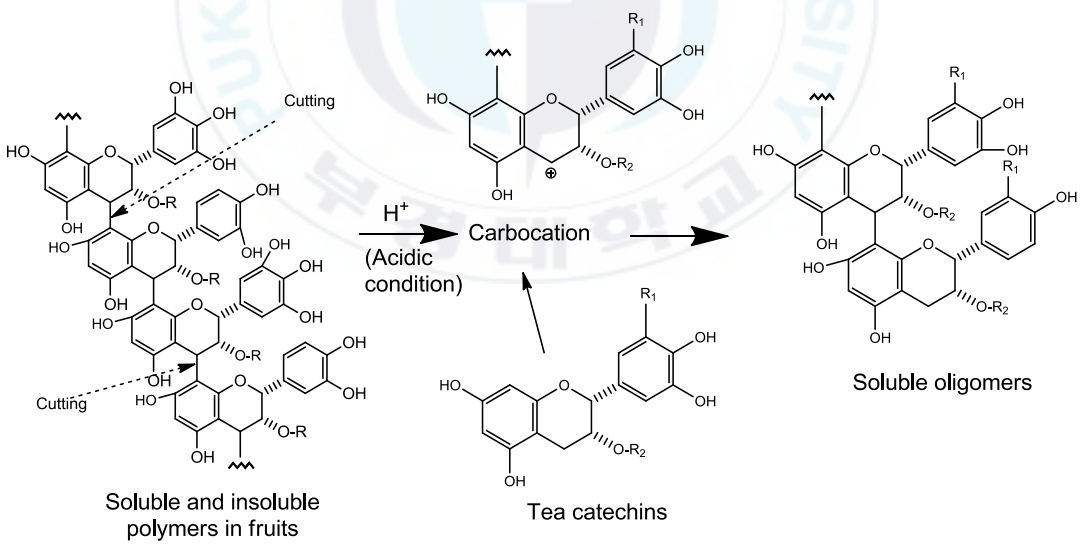

Fig. 2. Conversion of proanthocyanidin to low molecular weight oligomers.

Table 1. Phenol composition of oligonol used in the present study

Phenols	**Composition (%)**
Monomers (flavin-3-ols)	
Catechin + epicatechin	6.94
Epigallocatechin	1.36
Epigallocatechin gallate	7.02
Dimers (procyanidin)	
Procyanidin A1	6.21
Procyanidin A2	6.59
Procyanidin B1	0.43
Procyanidin B2	1.98
Epicatechin-epigallocatechin gallate	1.45
Trimers	
Epicatechin-procyanidin A2	4.53
Total of other phenolic compounds	54.98
Total polyphenols	91.49
Miscellaneous (water, proteins, fats, etc)	8.51

Oligonol comprise a polyphenol mixture of 15.3% monomers, 16.7% dimmers, and 4.53% trimers (Nonaka et al. 2004).

1.2. Chemicals and reagents

Yeast α-glucosidase, *p*-nitrophenyl α-D-glucopyranoside (pNPG), acarbose, *p*-nitrophenyl phosphate (pNPP), ursolic acid, ethylenediaminetetraacetic acid (EDTA), electric-eel AChE (EC 3.1.1.7), horse-serum BChE (EC 3.1.1.8), acetylthiocholine iodide (ACh), butyryl thiocholine chloride (BCh), 5,5'-dithiobis [2-nitrobenzoic acid] (DTNB), berberine, quercetin and diethylenetriamine penta acetic acid (DTPA), 2',7'-dichlorodihydrofluorescein diacetate (DCFH-DA), bovine serum albumin (BSA), Insulin from bovine pancreas, 6-hydroxy-2,5,7,8-tetramethylchroman-2-carboxylic acid (Trolox), Dimethyl sulfoxide (DMSO), 3-(4,5-dimethylthiazol-2-yl)-2,5-diphenyl tetrazolium bromide (MTT), *t*-BHP, bovine serum albumin, silymarin were purchased from Sigma-Aldrich (St. Louis, MO, USA). The fluorescent D-glucose analogue and glucose tracer 2-[N-(7-nitrobenz-2-oxa-1, 3-diazol-4-yl) amino]-2- deoxy-D-glucose (2-NBDG) was purchased from Life Technologies (Carlsbad, CA, USA). PTP1B (human recombinant) was purchased from Biomol® International LP (Plymouth Meeting, PA, USA), and dithiothreitol (DTT) was purchased from Bio-Rad Laboratories (Hercules, CA, USA). A BACE1 FRET assay kit (β-Secretase) was purchased from the Pan Vera Co. (Madison, WI, USA). Metformin (hydrochloride),

phenylmethylsulfonyl fluoride (PMSF), Peroxynitrite ($ONOO^-$) were purchased from Cayman Chemicals Co (USA). Minimum essential medium (MEM), penicillin-streptomycin, 0.25% trypsin-ethylenediaminetetraacetic acid (EDTA), fetal bovine serum (FBS), sodium pyruvate and nonessential amino acids were purchased from Gibco- BRL Life Technologies (Grand Island, NY, USA). Anti-nitrotyrosine (clone 1A6, mouse monoclonal primary antibody, IgG2b) and anti-mouse (horse radish peroxide conjugate, goat-polyclonal secondary antibody, IgG) were purchased from Millipore Co. (Temecula, CA, USA), and polyvinylidene fluoride (PVDF) membrane (Immobilon-P) was purchased from Millipore Co. (Billelica, MA, USA). Phospho-Akt (Ser473) (D9E) XP Rabbit mAb, Caspse-3 antibody, obtained from Cell Signaling Technology (Danvers, MA, USA). PTP1B (D-4), IRS1 (C-20) antibody, p-IRS-1 (Ser307), Akt1 (C-20), PI3-kinase p110 (D-4), p-PI3-kinase p85α (Tyr 508), ERK1 (K-23), p-ERK (E-4), β-Actin (C4) and all secondary antibodies were obtained from Santa Cruz Biotechnology (Dallas, TX, USA). Supersignal® West Pico Chemiluminescent Substrate was obtained from Pierce Biotechnology, Inc. (Rockford, IL, USA). All other reagents were, if not indicated otherwise, purchased from Sigma-Aldrich (St. Louis, MO, USA).

2. Methods

2.1. Determination of enzymatic anti-diabetic activities of oligonol

2.1.1. α-Glucosidase inhibitory activity assay

Enzyme inhibition studies were carried out spectrophotometrically in a 96-well microplate reader using a modified procedure reported by Li et al. (2005). A total of 60 μL of the reaction mixture containing 20 μL of 100 mM phosphate buffer (pH 6.8), 20 μL of 2.5 mM pNPG in the buffer, and 20 μL of the test sample dissolved in 10% dimethyl sulfoxide (DMSO) were added to each well, followed by the addition of 20 μL of α-glucosidase [0.2 U/mL in 10 mM phosphate buffer (pH 6.8)]. The plate was incubated at 37°C for 15 min, and then 80 μL of 0.2 mM sodium carbonate solution was added to stop the reaction. Immediately thereafter, the absorbance was recorded at 405 nm using a microplate spectrophotometer (VERSA max, Molecular Devices, Sunnyvale, CA, USA). The control contained the same reaction mixture, except that the same volume of phosphate buffer was added instead of the sample solution. Acarbose was also dissolved in 10% DMSO and used as a positive control. The percent (%) inhibition was calculated by using the following equation: % inhibition = [(A_c –

$A_s)/A_c] \times 100$, where A_c was the absorbance of the control and A_s was the absorbance of the sample. The inhibitory activity of oligonol against α-glucosidase was expressed in terms of the IC_{50} value (μg/mL required to inhibit the substrate, pNPG, by 50%), as calculated from the log-dose inhibition curve.

2.1.2. Protein tyrosine phosphatase 1B inhibitory activity assay

The inhibitory activity of oligonol against human recombinant PTP1B was evaluated using pNPP as a substrate (Cui et al. 2006). Forty microliters PTP1B enzyme [0.5 U diluted with a PTP1B reaction buffer containing 50 mM citrate (pH 6.0), 0.1 M NaCl, 1 mM EDTA, and 1 mM DTT] were added to each 96 well with or without the sample dissolved in 10% DMSO. The plate was pre-incubated at 37°C for 10 min, and then 50 μL of 2 mM pNPP in PTP1B reaction buffer was added. Following incubation at 37°C for 20 min, the reaction was terminated with the addition of 10 M NaOH. The amount of *p*-nitrophenyl produced after enzymatic dephosphorylation from pNPP was estimated by measuring the absorbance at 405 nm using a microplate spectrophotometer (VERSA max). The nonenzymatic hydrolysis of 2 mM pNPP was corrected by measuring the increase

in absorbance at 405 nm obtained in the absence of PTP1B enzyme. The inhibition percentage (%) was obtained by the following equation: % inhibition = $[(A_c - A_s)/A_c] \times 100$, where, A_c was the absorbance of the control and A_s was the absorbance of the sample. Ursolic acid was used as a positive control. The PTP1B inhibitory activity of oligonol was expressed in terms of the IC_{50} value (μg/mL required to inhibit the substrate, pNPP, by 50%), as calculated from the log-dose inhibition curve.

2.1.3. Kinetic analysis of oligonol against α-glucosidase and protein tyrosine phosphatase enzyme

In order to determine the kinetics of oligonol, two kinetic methods were used, the Lineweaver-Burk plot and the Dixon plot (Lineweaver and Burk 1934; Cornish-Bowden 1974). Inhibition mechanisms of each enzymatic inhibition at various concentrations of oligonol were evaluated by monitoring the effect of different substrate concentrations *via* the Dixon plot and the effect of different sample concentrations was evaluated *via* the Lineweaver-Burk plot. A Dixon plot for the inhibition of α-glucosidase by oligonol was obtained in the presence of different concentrations of pNPG substrate: 0.625 mM, 1.25 mM and 2.5 mM. A Lineweaver-Burk plot for the inhibition of α-glucosidase was obtained in the

presence of different oligonol concentrations: 125 μg/mL, 62.5 μg/mL, and 31.25 μg/mL. Similarly, a Dixon plot for PTP1B inhibition by oligonol was obtained in the presence of different concentrations of the pNPP substrate: 1 mM, 0.5 mM and 0.25 mM. The Lineweaver-Burk plot for the inhibition of PTP1B was obtained in the presence of different oligonol concentrations: 10 μg/mL, 1 μg/mL, and 0.1 μg/mL. Both enzymatic procedures applied the same α-glucosidase and PTP1B assay methods. The types of inhibition were determined by both methods, whereas inhibition constants (K_i) were determined by interpreting the Dixon plots, in which the value of the x-axis implies (K_i).

2.2. Determination of enzymatic anti-Alzheimer's disease activities of oligonol

2.2.1. *In vitro* cholinesterase (ChE) enzyme assay

The inhibitory activities of the ChEs were measured using the spectrophotometric method developed by Ellman et al. (1961). Acetylthiocholine iodide (ACh) and butyryl thiocholine chloride (BCh) were used as substrates to assay the inhibition of AChE and BChE, respectively. The reaction mixture

contained: 140 µL of sodium phosphate buffer (pH 8.0), 20 µL of test sample solution (final concentration; 100 µg/mL), and 20 µL of either AChE or BChE solution, which was mixed and incubated for 15 min at room temperature. Tested samples and the positive control (berberine) were dissolved in 10% DMSO. The reactions were initiated by the addition of 10 µL of DTNB and 10 µL of either ACh or BCh, respectively. The hydrolysis of ACh or BCh was monitored by tracking the formation of the yellow 5- thio-2-nitrobenzoate anion at 412 nm for 15 min, which resulted from the reaction of DTNB with thiocholine, released by the enzymatic hydrolysis of either ACh or BCh, respectively. All reactions were performed in triplicate and recorded in 96-well microplates, using a microplate spectrophotometer (VERSA max). Assays were carried out with a blank containing all components excepts AChE or BChE in order to account for non-enzymatic reaction. The enzyme solutions were prepared by dilution of the concentrated stock in phosphate buffer solution (0.1M, pH 8.0), as well as the stock sample solutions were diluted to a series of concentration with sodium phosphate buffer solution before the experiment. The percent (%) of inhibition was calculated by the following equation: % inhibition = (1-S/E) × 100, where S and E were the respective enzyme activities with and without the test sample,

respectively. The ChE inhibitory activity of each sample was expressed in terms of the IC_{50} value (μg/mL required to inhibit the hydrolysis of the substrate, ACh or BCh, by 50%), as calculated from the log-dose inhibition curve. The principle of cholinesterase inhibitory assay is shown in Fig. 3.

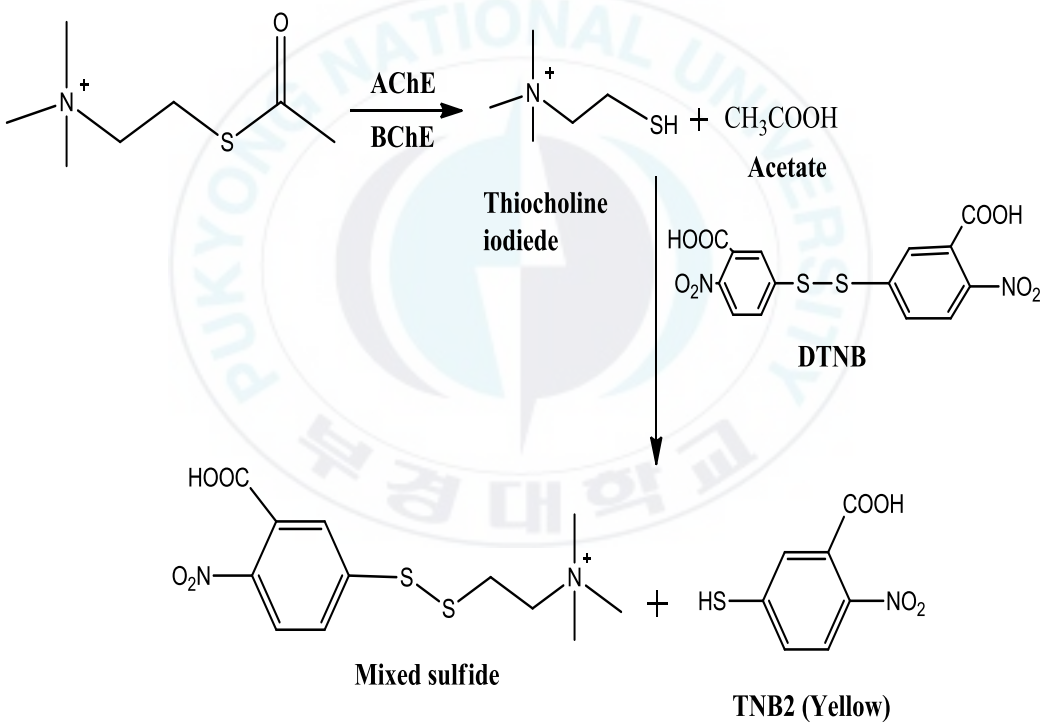

Fig. 3. The principle of cholinesterase inhibitory assay.

2.2.2. *In vitro* BACE1 enzyme assay

The assay was carried out according to the supplied protocol with select modifications (Jung et al. 2010; Choi et al. 2014). Oligonol activity was measured with a microplate spectrofluorometer (Gemini EM, Molecular Devices). Briefly, a mixture of 10 µL of the assay buffer (50 mM sodium acetate, pH 4.5), 10 µL of BACE1 (1.0 U/ml), 10 µL of the substrate (750 nM Rh-EVNLDAEFK-Quencher in 50 mM, ammonium bicarbonate), and 10 µL of the tested samples (final concentration: 250 µg/mL) dissolved in 10% DMSO was incubated for 60 min at 25°C in the dark. The proteolysis of two fluorophores (Rh-EVNLDAEFK-Quencher) by BACE1 was monitored by the formation of the fluorescent donor (Rh-EVNL), which increases in fluorescence at 530-545 nm (excitation) and 570-590 nm (emission). Fluorescence was measured with a microplate spectrofluorometer (Gemini EM, Molecular Devices, and Sunnyvale, CA, USA). The mixture was irradiated at 545 nm and the emission intensity was recorded at 585 nm. The percent inhibition (%) was obtained by the following equation: % inhibition = $[1-(S_{60}-S_0)/ (C_{60}-C_0)] \times 100$, where C_{60} was the fluorescence of the control (enzyme, buffer, and substrate) after 60 min of incubation, C_0 the initial fluorescence of the control, S_{60} the fluorescence of the tested samples (enzyme,

sample solution, and substrate) after 60 min of incubation, and S_0 the initial fluorescence of the tested samples. To allow for the quenching effect of the samples, the sample solution was added to the reaction mixture, and any reduction in fluorescence by the sample was then investigated. The BACE1 inhibitory activity of oligonol was expressed in terms of the IC_{50} value (μg/mL required to inhibit the proteolysis of the BACE1 substrate by 50%), as calculated from the log-dose inhibition curve. Quercetin was used as the positive control. The principle of the BACE1 inhibitory assay is shown in Fig. 4.

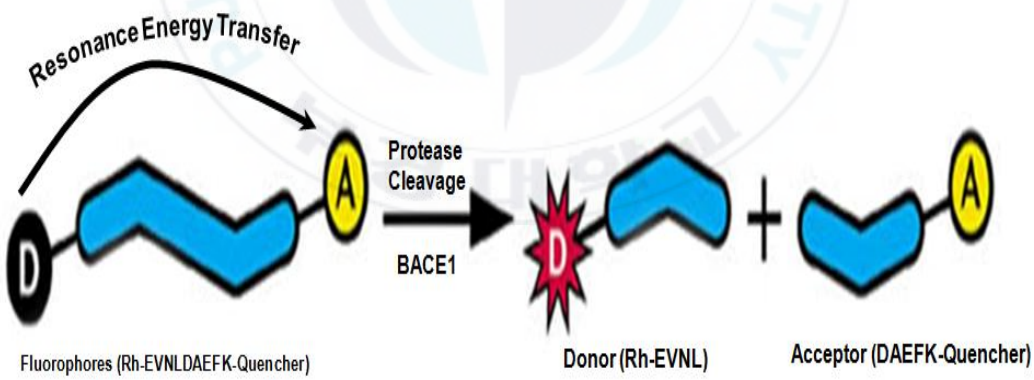

Fig. 4. Principle of the BACE1 inhibitory assay.

2.2.3. Kinetic parameters of oligonol in *in-vitro* ChE and BACE1 enzyme assays

The Dixon plot and Lineweaver-Burk plot were also used to determine the kinetic mechanism of oligonol against the ChEs and BACE1 enzyme (Lineweaver and Burk 1934; Cornish-Bowden 1974). Dixon plots for ChE and BACE1 inhibition were obtained in the presence of different concentrations of substrates ACh and BCh (0.6 mM, 0.3 mM, 0.15 mM) and of BACE1 substrate (150 nM, 250 nM, 375 nM). A Lineweaver-Burk plot for AChE and BChE inhibition was obtained in the presence of different concentrations of oligonol: 20 μg/mL, 4 μg/mL, 0.8 μg/mL, and 10 μg/mL, 1 μg/mL, 0 μg/mL, respectively. The Lineweaver-Burk plot for BACE1 inhibition was also obtained in the presence of different concentrations of oligonol: 250 μg/mL, 125 μg/mL, and 62.5 μg/mL. The modes of inhibition were determined by both methods, whereas inhibition constants (K_i) were determined by interpreting the Dixon plots. The enzymatic procedures consisted of the aforementioned ChEs and BACE1 assay methods.

2.3. Determination of antioxidant properties of oligonol.

2.3.1. Assay for $ONOO^-$ scavenging activity

The $ONOO^-$ Scavenging activity of oligonol was determined by the modified Kooy's method (Kooy et al. 1994), which involved monitoring highly fluorescent rhodamine 123 that was rapidly produced from non-fluorescent dihydrorhodamine (DHR) 123 in the presence of $ONOO^-$. In brief, the rhodamine buffer (pH 7.4) consisted of 50 mM sodium phosphate dibasic, 50 mM sodium phosphate monobasic, 90 mM sodium chloride, 5.0 mM potassium chloride, and 100 μM diethylenetriamine pentaacetate (DTPA). The final DHR 123 concentration was 5 μM. The assay buffer was prepared prior to use and placed on ice. Oligonol was dissolved in 10% DMSO. The background and final fluorescent intensities were measured 5 min after treatment with and without the addition of authentic $ONOO^-$ (10 μM) dissolved in 0.3 N sodium hydroxide (NaOH). The fluorescence intensity of the oxidized DHR 123 was evaluated using a fluorescence microplate reader (Bio-Tek Instruments Inc., FL×800, Winooski, UT, USA) at excitation and emission wavelengths of 480 and 530 nm, respectively. The values of the $ONOO^-$ scavenging activity was calculated as the

final fluorescence intensity minus the background fluorescence via the detection of DHR 123 oxidation. L-Penicillamine was used as the positive control.

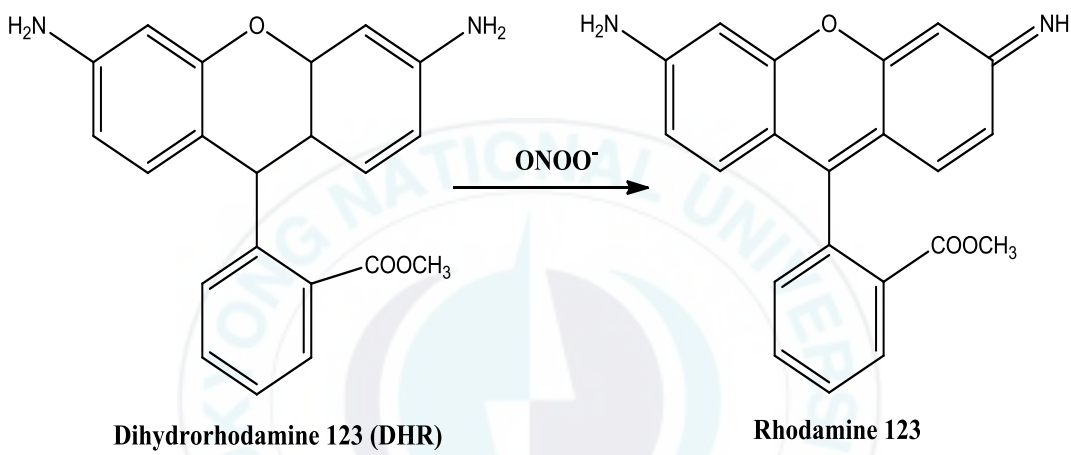

Fig. 5. The principle of $ONOO^-$ scavenging assay.

2.3.2. Inhibition of $ONOO^-$-mediated tyrosine nitration

$ONOO^-$-mediated protein tyrosine nitration was evaluated using the method of Jung et al. (2010) with slight modification. 2.5 μL of oligonol (final conc., 3.12 μg/mL, 6.25 μg/mL, and 12.5, μg/mL) dissolved in 10% DMSO was added to 95 μL of BSA (0.5 mg protein/mL). The mixtures were incubated at room temperature for 10 min and then mixed with 2.5 μL of $ONOO^-$ (200 μM). After incubation with shaking, the mixture sample was added to Bio-Red gel buffer in a ratio of 1:1 and boiled for 6 min to denature the proteins. The total protein equivalent for the reactant was separated on 10% SDS-polyacrylamide gel at 80V for 30 min, followed by 100V for 1 hour, and then electrophoretically transferred to polyvinylidene fluoride membrane at 80V for 110 min in a wet transfer system (Bio-Rad, Hercules, CA, USA). The membrane was immediately placed in a blocking solution (5% skim milk powder in TBS-Tween buffer containing 10 mM tris, 100 mM NaCl, and 0.1% Tween-20, pH 7.4) at room temperature for 2 h. The membrane was washed three times (10 min) in TBS-Tween buffer and incubated with a monoclonal anti-nitrotyrosine antibody (5% skim milk, diluted 1:2000 in TBS-Tween buffer) at 4 °C overnight. After two times washings in TBS-Tween buffer (10 and 5 min), the membrane was incubated with horseradish

peroxidase-conjugated antimouse secondary antibody (5% w/v skim milk) and diluted 1:2000 in TBS-Tween buffer at room temperature for 1 h. After two-time washing in TBS-Tween buffer (10 and 5 min), the antibody labeling was visualized with a super signal west pico chemiluminescent substrate (Pierce, Rockford, IL, USA) according to the manufacturer's instructions, and exposed to X-ray film (Kodak, Rochester, NY, USA). Pre-stained blue protein markers were used for molecular weight determination.

2.3.3. Assay for inhibition of total ROS generation.

The scavenging activity of oligonol against for the generation of ROS was assessed using the ROS-sensitive fluorescence indicator DCFH-DA (Lebel and Bondy 1990; Jung et al. 2009), a fluorescent oxidative stress indicator. The mixture of samples (concentration were 1.6, 8, and 40 μg/mL) and the post-mitochondrial fraction was then loaded with 50 μL of DCFH-DA (12.5 mM) in a potassium phosphate buffer and shaken for 5 min. The fluorescence of 2', 7'-dichlorodihydrofluorescein (DCF), the oxidation product of DCFH-DA, was measured at an excitation wavelength of 485 nm and an emission wavelength of 530 nm after 30 min on a microplate fluorescence spectrophotometer (FL × 800,

Bio-Tek Instruments, Inc). Trolox (same concentration) was used as the positive control. The principle of total ROS scavenging activity is shown in Fig. 6.

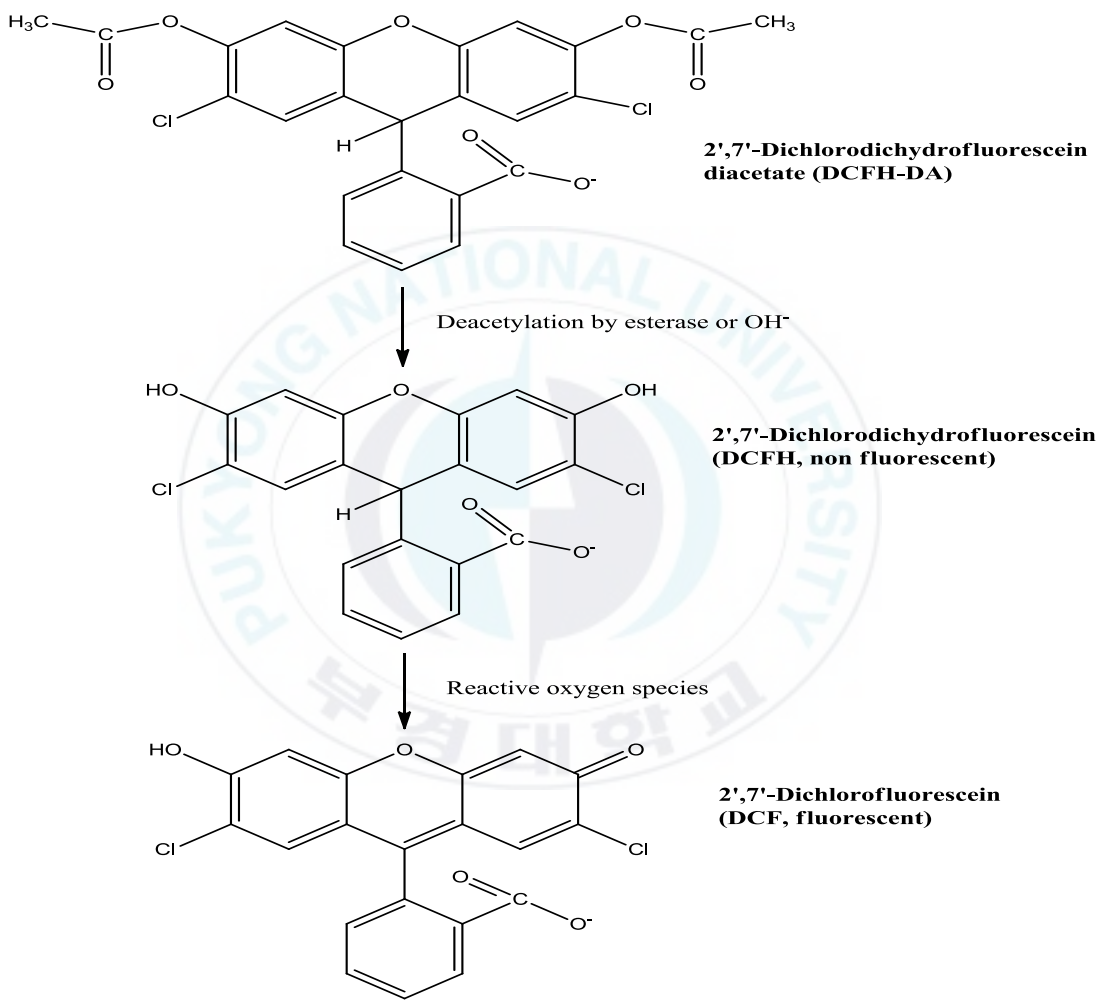

Fig. 6. Assay of the inhibitory activity on the ROS generation.

2.3.4. Measurement of intracellular ROS level

A fluorometric assay was used to determine the effects of oligonol on intracellular ROS generation in HepG2 cells applying the oxidant-sensitive fluorescence probe 2',7'-dichlorofluorescein diacetate (DCFH-DA) (Lebel and Bonday 1990). HepG2 cells were seeded in black 96 well plate at a density of 2×10^4 cells/well for 24 h and after 80% confluence incubated with oligonol at a different concentration range from 2.5 to 10 μg/mL for 2 h. Cells were then exposed to *t*-BHP (200 μM) to induced ROS production and subsequently incubated with DCFH-DA (20 μM) for 30 min. The resultant fluorescence intensities were measured at an excitation wavelength of 485 nM and an emission wavelength of 530 nM using a fluorescence microplate reader (FL × 800; Bio-Tek Instruments Inc., Winooski, UT, USA).

2.4. Cytoprotective assay of oligonol in HepG2 cells

2.4.1. Cell culture

The HepG2 (human hepatocarcinoma) cell line was purchased from American Type Culture Collection (HB-8065, Manassas, VA, USA). Cells were

maintained in minimum essential medium (MEM) containing 2.0 mM l-glutamine, 0.1 mM nonessential amino acids, 1.0 mM sodium pyruvate and 10% FBS at 37°C in a humidified atmosphere with 5% CO_2. The medium was changed every 48 h. Samples were dissolved in DMSO before being added to cells; the final concentration of DMSO did not exceed 0.1%.

2.4.2. Cell Viability Assay:

Cell viability was assessed using the MTT assay as previously described (Mossman 1983). In brief, HepG2 cells were seeded into a 96-well plate at a density of 2×10^4 cells per well and incubated at 37°C for 24 h. The cells were then fed with serum-free (SF-MEM) containing various concentrations (1, 10, 25, and 50 μg/mL) of oligonol, and then incubated for 24 hr or 48 h. After that cells were incubated with the addition of 100 μl of MTT solution 0.5 mg/mL in phosphate-buffered saline (PBS) followed by a 2 h incubation. To measure the proportion of surviving cells, the medium was replaced with 100 μl of DMSO (100%). Control cells were treated with 0.1% DMSO; this concentration exhibited no cytotoxicity as measured by this assay. The resultant absorbances at

570 nm were measured with a microplate reader (Molecular Devices, Sunnyvale, CA, USA).

2.4.3. *t*-BHP induced cytoprotective assay in HepG2 cells

Cytoprotective effects of oligonol against *t*-BHP induced oxidative damage were determined by an established method (Mossman et al. 1983). In brief, HepG2 cells were seeded into a 96-well plate at a density of 2×10^4 cells per well and incubated at 37°C for 24 h. The cells were then fed with SF-MEM containing various concentrations (2.5, 5 and 10 μg/mL) of oligonol, and incubated for 24 h. After 24 h, incubated with (SF-MEM) containing either *t*-BHP (200 μM). Cells were then incubated for 2 h, respectively, before the addition of 100 μl of MTT solution [0.5 mg/ml in phosphate-buffered saline (PBS)] followed by a 2 h incubation. To measure the proportion of surviving cells, the medium was replaced with 100 μl of DMSO (100%). Control cells were treated with 0.1% DMSO; this concentration exhibited no cytotoxicity as measured by this assay. The resultant absorbance at 570 nm was measured with a microplate reader (Molecular Devices, Sunnyvale, CA, USA).

2.5. Determination of antidiabetic activities in HepG2 cell lines

2.5.1. Glucose uptake to determine insulin concentration for resistance

The following protocol was used to determine the optimal dose of insulin and treatment duration required to establish insulin-resistant cells (Xie et al. 2006; Qin et al. 2011; Gao et al. 2015; Liu et al. 2015). Initially, 2 days prior to the experiment, the cells were seeded in 96-well plates (with 2×10^5 cells/well) with certain wells remaining empty. Second once the cells reached confluence 80%, the medium was replaced with SF-MEM supplemented with insulin at various concentrations (10^{-8}, 10^{-7}, 10^{-6} and 10^{-5} mol/L) for 36 h. Subsequently, the cells were treated with SF-MEM supplemented with insulin (10^{-6} mol/L) for 24, 48 and 72 h. At the end of the incubation periods, the medium was removed and glucose concentrations were determined using 2-NBDG. HepG2 cell glucose uptake was calculated by subtracting the glucose concentration of the wells with cells from the glucose levels of the blank wells. The established IR HepG2 cells were then treated with different concentrations of oligonol (2.5, 5, and 10 μg/mL) for 24 h and glucose uptake was determined as described below.

2.5.2. 2-NBDG Glucose Uptake.

HepG2 cells were routinely grown in MEM supplemented with 10% (v/v) fetal bovine serum, streptomycin (100 mg/mL), and penicillin (100 U/mL), in a humidified atmosphere of 95% air – 5% CO_2 at 37°C. The establishment of an insulin-resistant HepG2 cell model and glucose uptake was performed according to the reported method (Jung et al. 2011; Qin et al. 2011; Xie et al. 2006; Liu et al. 2015) with slight modifications. Briefly, HepG2 cells were cultured (with 2×10^4 cells/well) in 96-well cluster plates. After reaching confluence 80%, the cells were treated with 10^{-6} mol/L insulin for 24 h to induce insulin resistance, subsequently added at different concentrations of oligonol or metformin hydrochloride (no cytotoxic concentrations, see Fig. 14) and incubated for 24 h, and after that incubated with 100 nM insulin for 30 min. After this incubation, 2-NBDG uptake in insulin-resistant HepG2 cells was measured. The cells were incubated with 40 μM 2-NBDG (dissolved in PBS with 1% BSA) for 20 min. To stop the response, cells were washed 3 times with ice-cold 1XPBS and the fluorescence intensity of 2-NBDG was measured on a fluorescence microplate reader (Bio-Tek Instruments Inc., FL×800, Winooski, UT, USA) at 485 nm

excitation and 528 nm emission. Five replicate wells were established, and each experiment was repeated three times.

2.5.3. Preparation of cell lysates and western blot analysis:

Insulin-resistant HepG2 cells (3×10^5 cells/well) in six-well plates were treated with different concentration oligonol for 24 h. After stimulating with 100 nM insulin for 30 min at 37°C, the cells were washed 2 times with ice-cold 1XPBS and collected, then lysed with sample buffer (50 mM Hepes pH 7.5, 150 mM NaCl, 2.5 mM EDTA, 0.5% NP-40, 1 mM PMSF, 1 mM DTT, 0.2% aprotinin,0.5 % leupetin, 20 mM NaF and 1 mM Na_3VO_4) on ice. After incubation on ice for 30 min, insoluble materials were removed by centrifugation at 25, 000 × g for 20 min. The protein concentrations were determined by Modified Bradford protein assay kit using BSA as a standard and then stored at-80°C until used for Western blotting analyses. Protein samples from insulin-resistant HepG2 cells were separated by 10% sodium dodecyl sulfate-polyacrylamide gel electrophoresis (SDS-PAGE) and transferred to a polyvinylidene difluoride (PVDF) membrane (Immobilon-P; Millipore, Burlington, MA, USA). The membranes were blocked with 5% skim milk in 1 ×

Tris-buffered saline containing 0.1% Tween 20 (TBST) for 2 hr at room temperature and were then incubated 18th h at 4°C with a primary antibody. The following day, the membranes were washed with TBST for 30 min and were probed with a secondary antibody for 2-3 h. The bands were detected using the Supersignal west Pico chemiluminescence substrate (Pierce) according to the manufacturer's instruction. Protein bands were visualized by X-ray film (Kodak, Rochester, NY). Prestained blue protein markers were used for molecular weight determination.

2.6. Molecular docking simulation in PTP1B inhibition

Docking study was performed to examine qualified binding poses for the constituents of oligonol against PTP1B. An X-ray crystallographic structure of potent, selective PTP1B inhibitor compound 23 using a linked-fragment strategy (PDB ID: 1NNY) at a resolution of 2.40 Å (Szczepankiewicz et al. 2003) was obtained from the RCSB protein data bank (Bernstein et al. 1977; Berman et al. 2002). For docking simulations, the 515 heteroatoms were removed, the protein was regarded as ligand-free, and water molecules were also removed from the protein structure using Accelrys Discovery Studio 4.1 (DS 4.1) (DS,

http://www.accelrys.com; Accelrys, Inc. San Diego, CA, USA). Polar hydrogen atoms were added to the protein using the automated docking tool Autodock 4.2 (Goodsell et al. 1996; Jones et al. 1997; Rarey et al. 1996). For docking studies, the 515 binding area of the protein was considered as the most likely region for docking simulation with respect to obtaining the best results for ligand binding. The 3D structure of the constituents of oligonol was obtained from the PubChem compound (NCBI). We used Autodock 4.2 for docking simulation, which is an open source program for doing molecular docking and significantly improves the average accuracy of the binding mode predictions compared to Autodock 4 (Trott and Olson 2010). A grid box size of 126× 126 × 126 points with a spacing of 0.375 Å between grid points was generated to cover almost the entire favorable protein binding site. The X, Y, and Z centers were 37.303, 30.97, and 33.501, respectively. The binding aspects of PTP1B residues and their corresponding binding affinity scores were regarded as the best molecular interactions. Results were analyzed using UCSF Chimera (http://www.cgl.ucsf.edu/chimera/; Pettersen et al. 2004) and Lig plus (V.1.4.5). Two-dimensional figures of the constituents of oligonol–PTP1B interactions were groomed using Lig plus (V.1.4.5). All

docking simulations were performed using an Intel® Core ™ i5-2520M CPU @ 2.50 GHz with Windows 8.1 and 64bit operating system.

2.7. Statistical analysis.

The significance of differences between the control and test groups was determined by statistical testing using Student's *t*-test. All results are expressed as means ± standard errors of the mean (SEM) derived from triplicate experiments. The differences between groups, and ###$p < 0.001$, *$P < 0.05$, **$P < 0.01$, and ***$P < 0.001$ were determined by a one-way analysis of variance.

III. Results and Discussions

Part 1. Enzymatic inhibitory potential of oligonol

1.1. α-glucosidase and PTP1B inhibitory activities of oligonol

In order to evaluate the antidiabetic activity of oligonol, the inhibitory potential of α-glucosidase and PTP1B was evaluated using pNPG and pNPP as substrates, respectively, and results were expressed as IC_{50} values (concentration required to decrease α-glucosidase and PTP1B by 50%), which are presented in Table 2. Oligonol showed concentration-dependent inhibitory activity against α-glucosidase and PTP1B (Fig. 7AB). Notably, oligonol exhibited the most potent PTP1B inhibitory potential with an IC_{50} value of 1.02 ± 0.04 μg/mL compared to the positive control, ursolic acid, with an IC_{50} value of 1.62 ± 0.02 μg/mL (Table 2, Fig. 7B). In addition, oligonol also displayed 5-fold stronger α-glucosidase inhibitory activity with an IC_{50} value of 23.14 ± 0.91 μg/mL, compared to the positive control, acarbose, with an IC_{50} value of 116.73 ± 2.72 μg/mL (Table 2, Fig. 7A).

Table 2. Enzyme kinetics analysis of the anti-diabetic activities of oligonol

	α-Glucosidase	PTP1B
IC_{50} (μg/mL) [a]	23.14 ± 0.91	1.02 ± 0.04
K_i [b]	22.36	8.51
Inhibition type [c]	Mixed	Mixed
Acarbose [d]	116.73 ± 2.72	
Ursolic acid [e]		1.62 ± 0.02

[a] 50% inhibition concentrations are expressed as the mean ± SEM of both experiments.
[b] The inhibition constants (K_i) were determined by interpreting the Dixon plot.
[c] Inhibition type was determined by interpreting the Dixon and Lineweaver-Burk plots.
[d,e] 50% inhibition concentrations of acarbose and ursolic acid were used as positive controls for α-glucosidase and PTP1B assays, respectively.

A

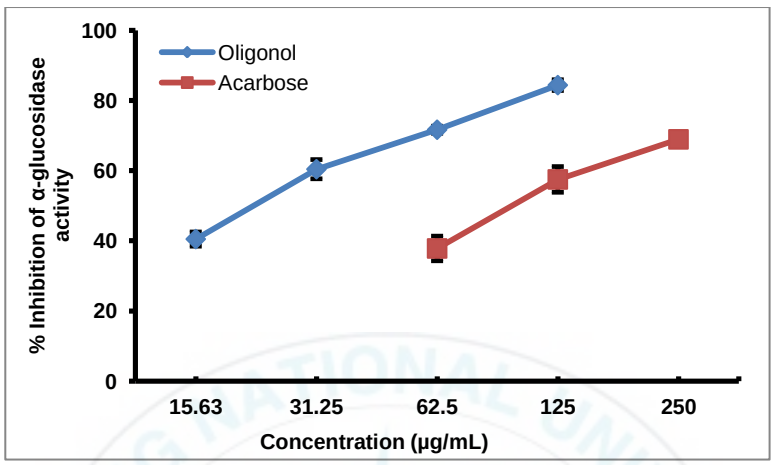

B

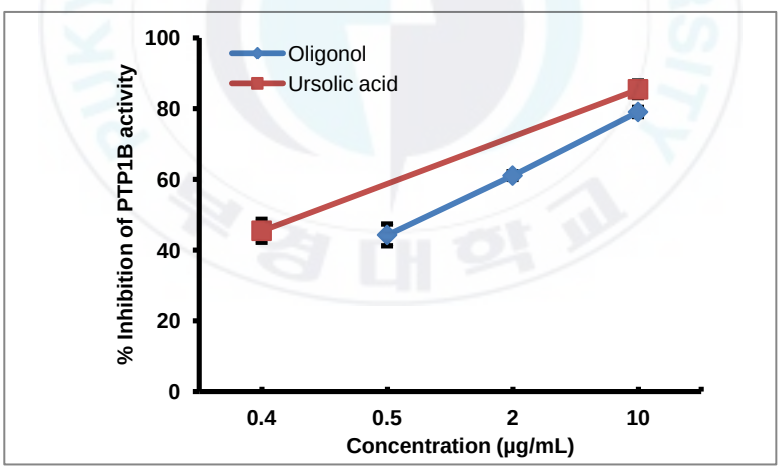

Fig. 7. Concentration-dependent inhibitory activity of oligonol and acarbose on α-glucosidase (**A**) and oligonol and ursolic acid on PTP1B (**B**) was analyzed in the presence of different sample concentrations, as follows: 125 μg/mL; 62.5 μg/mL; 31.25 μg/mL; 15.63 μg/mL, and 10 μg/mL; 2 μg/mL; 0.5 μg/mL, respectively.

1.2. Kinetic studies of oligonol's α-glucosidase and PTP1B inhibition

Since the results from the inhibition assays demonstrated that oligonol displayed strong inhibition against α-glucosidase and PTP1B, the inhibition mechanism of both enzymes was further determined using enzyme kinetic analyses. In an attempt to explain the mode of enzymatic inhibition, kinetic analyses were performed at different concentrations of the corresponding substrate (pNPG for α-glucosidase and pNPP for PTP1B) and various oligonol concentrations (Fig. 8AB, 9AB). Dixon and Lineweaver–Burk plots were drawn using the data obtained from the kinetic studies in order to confirm the inhibition pattern and the inhibition constants (K_i) were determined by interpretation of Dixon plots (Table 2; Fig. 8.AB, and Fig. 9AB). Concentration of pNPG is denoted by (A): 2.5 mM (*filled circle*); 1.25 mM (*empty circle*); 0.625 mM (*filled inverted triangle*), and concentration of pNPP by (B): 1 mM (*filled circle*); 0.5 mM (*empty circle*); 0.25 mM (*filled inverted triangle*), which are shown to intersect on the left side, indicating mixed-type inhibition against α-glucosidase and PTP1B with K_i values of 22.36 and 8.52, respectively (Fig. 8A for α-glucosidase; Fig. 8B for PTP1B). In the Lineweaver–Burk plots, various concentration lines of oligonol (A); 125 μg/mL (*filled circle*); 62.5 μg/mL (*empty*

circle); 31.25 μg/mL (*filled inverted triangle*), for α-glucosidase and (B); 10 μg/mL (*filled circle*); 1 μg/mL (*empty circle*); 0.1 μg/mL (*filled inverted triangle*), for PTP1B, are also shown to intersect on the left side, indicating mixed type inhibition against α-glucosidase and PTP1B (Fig. 9A for α-glucosidase; Fig. 9B for PTP1B).

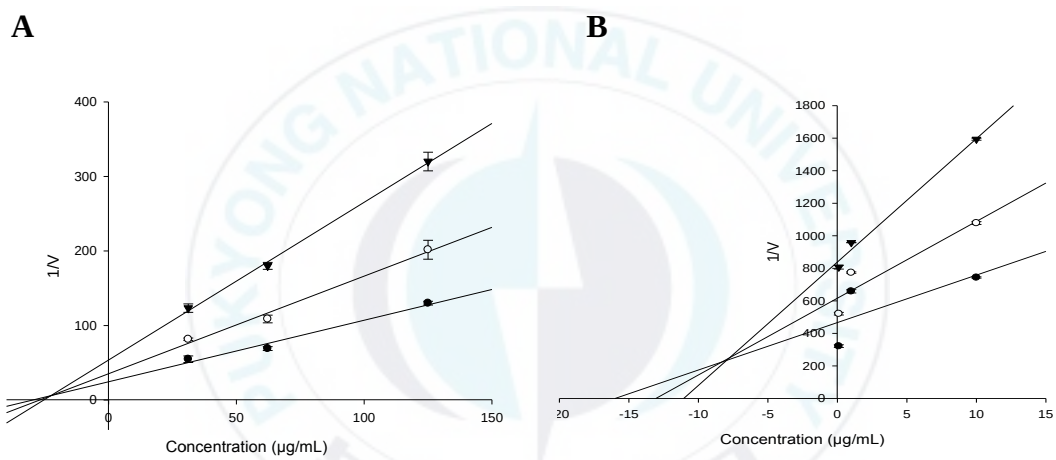

Fig. 8. Dixon plot for α-glucosidase (**A**) and PTP1B (**B**) inhibition of oligonol, tested in the presence of different substrate concentrations of *p*-nitrophenyl α-D-glucopyranoside: 2.5 mM (*filled circle*); 1.25 mM (*empty circle*); 0.625 mM (*filled inverted triangle*), and *p*-nitrophenyl phosphate: 1 mM (*filled circle*); 0.5 mM (*empty circle*); 0.25 mM (*filled inverted triangle*), respectively.

A

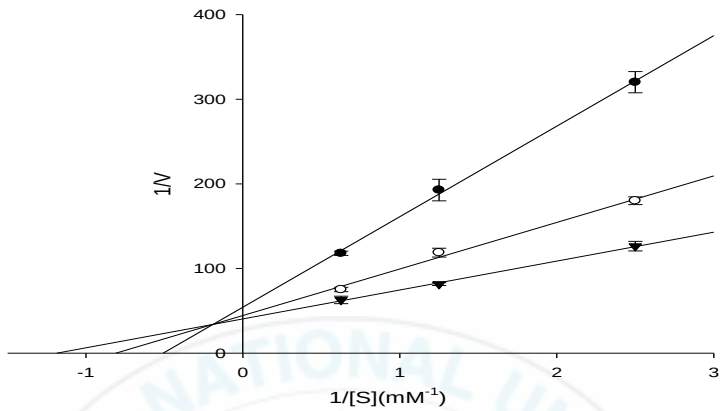

B

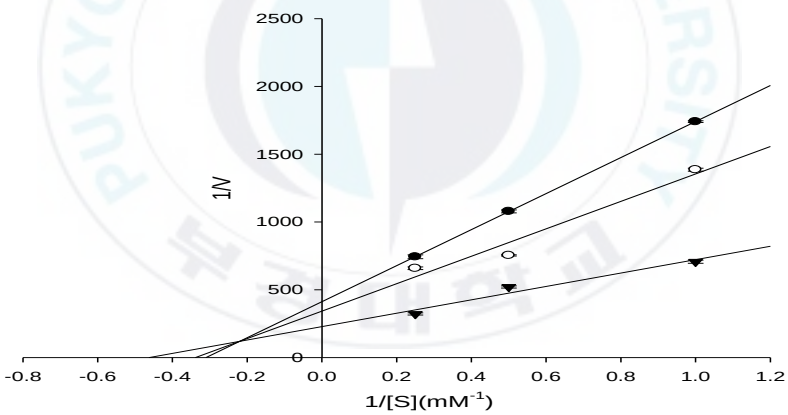

Fig. 9. Lineweaver-Burk plot for α-glucosidase (**A**) and PTP1B (**B**) inhibition of oligonol, analyzed in the presence of different sample concentrations, as follows: 125 μg/mL (*filled circle*), 62.5 μg/mL (*empty circle*), 31.25 μg/mL (*filled inverted triangle*), and 10 μg/mL (*filled circle*), 1 μg/mL (*empty circle*), 0.1 μg/mL (*filled inverted triangle*), respectively.

1.3. Anti-Alzheimer potential of oligonol

1.3.1. Inhibitory activities of oligonol against AChE, BChE, and BACE1.

Since acetylcholine decline and Aβ formation is potentially involved in the pathogenesis of AD (Butterfield et al. 2001), oligonol's inhibitory activity against cholinesterase (both AChE and BChE) and BACE1 enzymes was evaluated. The results obtained in different assays are summarized in Table 3. Oligonol showed potent inhibitory activities against AChE and BChE in a concentration-dependent manner with IC_{50} values of 4.34 ± 0.06 μg/mL and 2.07 ± 0.53 μg/mL, respectively, compared to the positive control, berberine, with IC_{50} values of 0.01 ± 0.002 μg/mL and 0.67 ± 0.02 μg/mL, respectively (Table 3, Fig. 10AB). In the case of the BACE1 assay, oligonol showed concentration-dependent moderate inhibitory activities with an IC_{50} value of 130.45 ± 1.49 μg/mL, compared to the positive control, quercetin, with an IC_{50} value of 6.81 ± 0.15 μg/mL (Table 3, Fig. 10C).

Table 3. Enzyme kinetics analysis of the anti-Alzheimer activities of oligonol

	AChE	BChE	SI [f]	BACE1
IC_{50} (μg/mL) [a]	4.34 ± 0.06	2.07 ± 0.53	0.48	130.45 ± 1.49
K_i [b]	4.65	9.80		58.80
Inhibition type [c]	Mixed	Noncompetitive		Mixed
Berberine [d]	0.01 ± 0.002	0.67 ± 0.02		
Quercetin [e]				6.81 ± 0.15

[a] 50% inhibition concentrations are expressed as the mean ± SEM of triplicate experiments.
[b] The inhibition constants (K_i) were determined by interpreting the Dixon plot.
[c] Inhibition types were determined by interpreting Dixon and Lineweaver-Burk plots.
[d,e] 50% inhibition concentrations of berberine and quercetin were used as positive controls for ChE and BACE1 assays, respectively.
[f] Selective index (BChE/AChE).

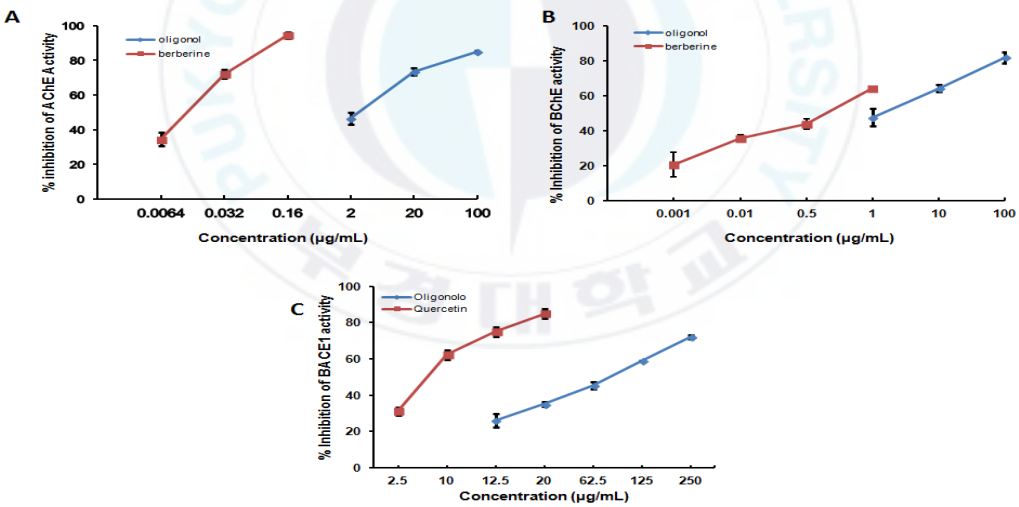

Fig. 10. Concentration-dependent inhibitory activity of oligonol and berberine on AChE (**A**) and BChE (**B**) and oligonol and quercetin on BACE1 (**C**) were analyzed in the presence of different sample concentrations, as follows: 100 μg/mL; 20 μg/mL; 2 μg/mL, 100 μg/mL; 10 μg/mL; 1 μg/mL and 250 μg/mL; 125 μg/mL; 62.5 μg/mL; 12.5 μg/mL, respectively.

1.3.2. Kinetic studies of oligonol for AChE, BChE, and BACE1

The mechanism of inhibition of ChEs and BACE1 enzymes was further determined using enzyme kinetic analyses. In an attempt to explain the mode of enzymatic inhibition, kinetic analyses were performed at different concentrations of the corresponding substrate (ACh for AChE, BCh for BChE and BACE1 substrate for BACE1) and various oligonol concentrations (Fig. 11, 12). In the Dixon plot, various concentration lines of ACh (A); 0.15 mM (*filled inverted triangle*); 0.3 mM (*empty circle*); 0.6 mM (*filled circle*), and BACE1 substrate (C): 150 nM (*filled inverted triangle*); 250 nM (*empty circle*); 375 nM (*filled circle*) were shown to intersect on the left side, indicating mixed-type inhibition of AChE and BACE1 with Ki values 4.65 and 58.80, respectively (Fig; 11A for AChE; Fig. 11C for BACE1). Meanwhile the concentration lines of BCh (B); 0.15 mM (*filled inverted triangle*); 0.3 mM (*empty circle*); 0.6 mM (*filled circle*), showed the same x-intercept, suggesting that oligonol functions as a noncompetitive inhibitor against BChE (Fig. 11B). These results are similar to those of the Lineweaver-Burk plots, where various concentration lines of oligonol (A); 20 μg/mL (*filled circle*); 4 μg/mL (*empty circle*); 0.8 μg/mL (*filled inverted triangle*), for AChE and (B): 10 μg/mL (*filled circle*); 1 μg/mL (*empty circle*); 0

μg/mL (*filled inverted triangle*) for BChE, and (C); 250 μg/mL (*filled circle*); 125 μg/mL (O); 62.5 μg/mL (*filled inverted triangle*) for BACE1, were found to demonstrate mixed-type inhibition against AChE, BACE1 and noncompetitive inhibition against BChE (Fig. 12ABC).

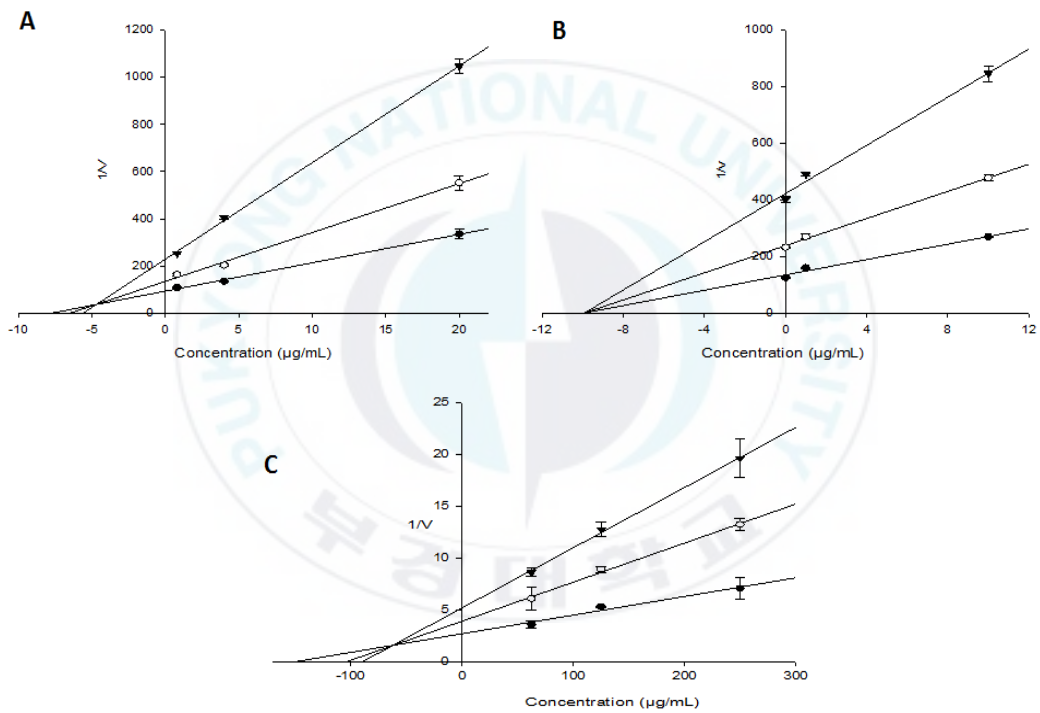

Fig. 11. Dixon plot for AChE (**A**), BChE (**B**) and BACE1 (**C**) inhibition of oligonol, tested in the presence of different substrate concentrations of acetyl thiocholine: 0.15 mM (*filled inverted triangle*); 0.3 mM (*empty circle*); 0.6 mM (*filled circle*), butyryl thiocholine: 0.15 mM (*filled inverted triangle*); 0.3 mM

(*empty circle*); 0.6 mm (*filled circle*), and BACE1: 150 nM (*filled inverted triangle*); 250 nM (*empty circle*); 375 nM (*filled circle*), respectively.

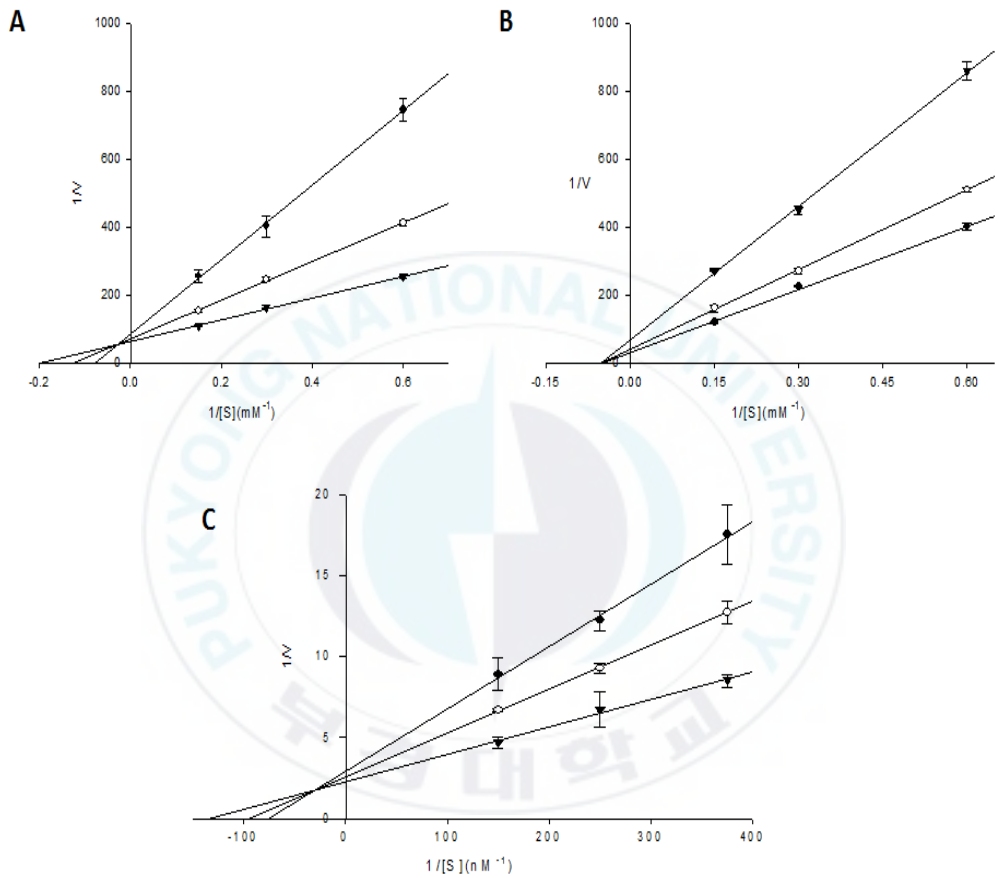

Fig. 12. Lineweaver-Burk plot for AChE (**A**), BChE (**B**) and BACE1 (**C**) inhibition of oligonol, analyzed in the presence of different sample concentrations, as follows: 20 μg/mL (*filled circle*), 4 μg/mL (*empty circle*), 0.8 μg/mL (*filled inverted triangle*), 10 μg/mL (*filled circle*), 1 μg/mL (*empty circle*), 0 μg/mL (*filled inverted triangle*), and 250 μg/mL (*filled circle*), 125 μg/mL (*empty circle*), 62.5 μg/mL (*filled inverted triangle*), respectively.

1.4. Inhibitory effect of oligonol on $ONOO^-$-mediated protein tyrosine nitration

The inhibitory activities of oligonol against $ONOO^-$-induced protein tyrosine nitration was determined via western blot analysis using the 3-nitrotyrosine antibody. As shown in Fig. 13, pretreatment with oligonol at different concentrations (3.12 μg/mL, 6.25 μg/mL, and 12.5 μg/mL) resulted in dose-dependent inhibitory activities against $ONOO^-$-mediated tyrosine nitration.

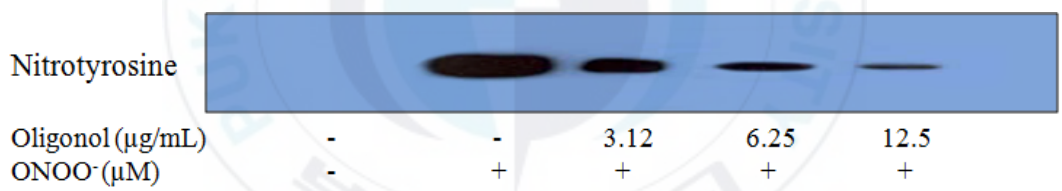

Fig. 13. Effects of oligonol on the nitration of BSA by $ONOO^-$. The mixtures of oligonol, BSA, and $ONOO^-$ were 37^0 C for 30 min. The reactant was resolved by electrophoresis in 10% SDS-polyacrylamide gel.

1.5. Discussion

Oligonol, derived from lychee fruit (85%) and green tea (15%), is the world's first "low molecular weight polyphenol" (Miura et al. 2010). Oligonol has comprised of a polyphenol mixture of 15.3% monomers (including catechin) and 16.7% dimers (including procyanidin and catechin), whereas lychee fruit polyphenol is comprised of a mixture of 6.4% monomers and 9.8% dimers (Park et al. 2015). Oligonol from lychee is characterized by unparalleled bioavailability and clinically proven efficacy and has extremely good absorption and wider anti-oxidant, anti-inflammatory and anti-aging actions than general polyphenol extract (Nishioka et al. 2006; Tomobe et al. 2007; Kundu et al. 2008; Sakurai et al. 2008). It was added as a new dietary ingredient from the US Food and Drug Administration (FDA) in 2007 and was generally recognized as safe by the FDA in 2014 (Fujii et al. 2008; Kitadate et al. 2014).

This study investigated the effects of oligonol on DM and AD. The results of the present study are consistent with previously reported results. According to reported studies, oligonol has been investigated as complementary agents because of their potential beneficial effects on health (Fujii et al. 2008; Kitadate et al. 2014). Some of the studies found that oligonol improves insulin resistance (Park

et al. 2015), as well as, may help to protect against certain diabetes-related complications (Noh et al. 2010, 2011; Park et al. 2015). In order to evaluate the antidiabetic activity of oligonol, its inhibitory potential against α-glucosidase and PTP1B was evaluated using pNPG and pNPP as a substrate, respectively, and results were expressed as IC_{50} values, which are presented in Table 2. During persistent hyperglycemia, α-glucosidase present in the brush border of the small intestine breaks down starch and disaccharides to glucose, which then can be absorbed quickly into the bloodstream. Hence, α-glucosidase inhibitors prolong the overall carbohydrate digestion time, and thus cause a reduction in the rate of glucose absorption and lower the postprandial rise in blood glucose (Kim et al. 2000; Standl and Schnell 2012). Therapeutic strategies focusing on the suppression of postprandial hyperglycemia and improving insulin signaling would, therefore, be valuable in the treatment of both diabetic patients and individuals with impaired glucose tolerance, making oligonol our α-glucosidase inhibitor drug of choice. Insulin receptors (IR), a subclass of a large family of protein tyrosine kinases, undergo autophosphorylation by binding insulin. This insulin-related event enhances IR kinase activity and triggers downstream signaling events, consequently eliciting most of the metabolic actions of insulin,

including glucose transport, glycogen synthesis, and inhibition of gluconeogenesis (Pessin and Saltiel 2000). On the other hand, PTP1B plays a crucial role in the negative regulation of a series of insulin's actions by dephosphorylating activated IR. It has been hypothesized that a specific protein tyrosine phosphatase is involved in the dephosphorylation and inactivation of the IR, which attenuates insulin signaling, and disequilibrium among the insulin receptor and protein tyrosine phosphatase could be a contributing factor to the insulin resistance observed in type 2 diabetes mellitus (Johnson et al. 2002). Among the available therapeutic approaches, inhibition of α-glucosidase and PTP1B has emerged as a potential therapeutic target for the treatment and prevention of type 2 diabetics mellitus (Kusari et al. 1994; Johnson et al. 2002). Apart from the currently available anti-diabetic drugs, several herbal medicines have also been recommended for the treatment of diabetes since they have fewer side effects compared to the modern therapeutic drugs (Ayodhya et al. 2010).

As a part of our continuous search for therapeutic agents from natural sources for diabetes and diabetic complications, we investigated the inhibitory potential of oligonol against α-glucosidase and PTP1B. To the authors' knowledge, no previous study has explained the α-glucosidase and PTP1B inhibitory activity of

oligonol (Table 2). We hence investigated the in vitro α-glucosidase and PTP1B inhibitory activity of oligonol with enzyme kinetics analyses for the first time (Fig. 7, 8, 9). In our study, oligonol proved to be a potent PTP1B inhibitor, compared to ursolic acid, as well as a significant α-glucosidase inhibitor, compared to the acarbose. In an attempt to explain the mode of inhibition of oligonol against α-glucosidase and PTP1B, we performed kinetic analyses at different concentrations of the substrate and various concentrations of oligonol. In the kinetics studies, oligonol showed mixed-type inhibition against α-glucosidase and PTP1B with K_i values 22.36 and 8.51, respectively. As the lower K_i value of oligonol against PTP1B implies tighter binding with the free enzyme PTP1B or the enzyme-substrate complex compared to binding with the α-glucosidase enzyme or the enzyme-substrate complex, which may explain the more potent inhibition of PTP1B and be important in the development of preventive and therapeutic agents. In conclusion, oligonol showed anti-diabetic activity may be via α-glucosidase and PTP1B pathways.

Two major hypotheses have been proposed regarding the molecular mechanism of the pathogenesis of AD: the cholinergic hypothesis and the amyloid cascade hypothesis. In order to treat and prevent AD, most

pharmacological research has focused on AChE and BChE inhibitors to alleviate the cholinergic deficit and to improve neurotransmission (Rao et al. 2007). AChE is the main enzyme responsible for the hydrolysis of the ACh at the cholinergic synapses while BChE acts as a co-regulator of the activity of AChE. Under normal physiological condition maximum cholinesterase activity is due to AChE however as the disease progresses AChE activity decreases in specific brain regions, whereas BChE activity increases which compensate some of the functions of AChE in cholinergic neurons. Consequently, therapeutic agents that serve as inhibitors of both these enzymes could provide additional benefits in AD (Kwon et al. 2010). Furthermore, BACE-1 which is involved in the first and rate-limiting step of Aβ formation from its APP has also generated great interest and nowadays several BACE-1 inhibitors are in clinical trials (Evin et al. 2011). Since Aβ results from the proteolysis of APP by Aβ and γ-secretases and the formation and accumulation of Aβ is crucial in AD pathogenesis, the BACE has recently emerged as a prevalent therapeutic target for AD. In as much as the consistent ratio of BChE to AChE, selective BChE inhibition, and BACE1 inhibition is key factors in the treatment of AD, it is important for AD therapies to inhibit both ChEs and BACE1 (Rao et al. 2007).

To evaluate the potential of oligonol as an anti-Alzheimer agent, ChE, and BACE1 inhibitory activity was measured using the modified method of Ellman et al. (1961), and the manufacturer's protocol, respectively. It is evident from Table 3 that oligonol exhibited potent inhibitory activity against both types of ChEs (AChE and BChE) while oligonol showed weak inhibitory activity against BACE1 (Fig. 10). However, based on the remarkable effect of oligonol *in vitro* ChEs assays compared to the lower than expected inhibitory activity against the BACE1 it is likely that the ameliorative activity of oligonol upon memory dysfunction depends on its ChEs inhibitory activity. In the kinetics studies, oligonol showed mixed-type inhibition against AChE and BACE1 with respective K_i values of 4.56 and 58.80, whereas oligonol showed noncompetitive-type inhibition against BChE with a K_i value 9.80 (Fig. 11, 12). The K_i value of the ChEs kinetics analysis implies tighter binding with the free ChE enzyme or the enzyme-substrate complex. However, the K_i value of the BACE1 kinetics analysis implies a weaker binding with the BACE1 enzyme or enzyme substrate complex compared to the ChE kinetics analysis, which suggests that oligonol may act as a more effective inhibitor against ChEs. We hence investigated in vitro ChE and BACE1 inhibitory activity for the first time, with enzyme kinetics

analyses of oligonol. In the context of the relationship between the content of oligonol and efficacy against AChE and BACE1, it was speculated that the material with the highest content of oligonol would possess the strongest ChEs and BChE inhibitory activities. The superior effect of oligonol is due to the catechin-type monomers and the content of more bioavailable oligomeric proanthocyanidins. Till now the exact mechanism of actions is unknown. Previous studies showed that, oligonol improve memory and cognition on Alzheimer's mouse model (Choi et al. 2014), as well as, attenuated Aβ-induced cytotoxicity, apoptotic features, intracellular ROS accumulation, lipid peroxidation and increased the cellular glutathione pool both in vivo and in vitro (Li et al. 2004; Choi et al. 2014). Consistent with previous studies, oligonol exerted inhibitory effects on ChEs, and BACE1 enzymes in the present study, hypothesized that oligonol showed most potent anti-Alzheimer activity, may be via the ChEs pathway than the BACE1 pathway. Increasing evidence suggests that oxidative damage to proteins and other macromolecules are a salient feature of the pathology of diabetes mellitus and Alzheimer's disease. Tyrosine nitration is one specific form of protein oxidation that is associated with DM and AD (Smith et al. 1997; Reddy et al. 2009). $ONOO^-$ generation and the subsequent

nitrotyrosine formation could be promoted in diabetic by hyperglycemia and also affect the energy status of neurons as well as cell cycle by inactivating key enzymes (Ceriello et al. 2001; Rosales-Corral et al. 2015). Therefore, oligonol showed inhibitory activities against $ONOO^-$-mediated tyrosine nitration in a concentration-dependent manner (Fig. 13). Our result demonstrates that the nitrotyrosine inhibition of oligonol might participate in anti-diabetic and anti-Alzheimer activities. In conclusion, oligonol, which is now available commercially as a new dietary ingredient, is an optimized phenolic product derived from lychee fruit. In the present study, the anti-diabetic and anti-Alzheimer effects of oligonol were examined using several in vitro experiments. Oligonol was found to be a potential candidate for the treatment of DM and AD as well as their complications by inhibiting α-glucosidase, PTP1B, ChE and BACE1 activity, as well as inhibiting the $ONOO^-$-mediated tyrosine nitration mechanism. Thus, oligonol should be further explored for the development of novel therapeutic or preventive agents for the treatment of DM and AD.

Part 2. Oligonol promotes glucose uptake and protects hepatocyte by modulating the insulin signaling pathway in insulin-resistant HepG2 cells via PTP1B Inhibition.

2.1 Cytotoxicity of oligonol in HepG2 cells

To identify the cytotoxic effects of oligonol on HepG2 cells, the cells were treated with various concentrations of oligonol range 0 to 50 μg/ml for 24 and 48 h. Cell viability did not decrease below 90 % of the control level after 48 h, which was determined by the MTT assay. Our result found that the tested concentrations of oligonol did not grossly affect cell growth and viability (Fig. 14). Because the tested concentrations did not induce cytotoxicity, 2.5, 5, and 10 μg/mL of oligonol was used for further studies.

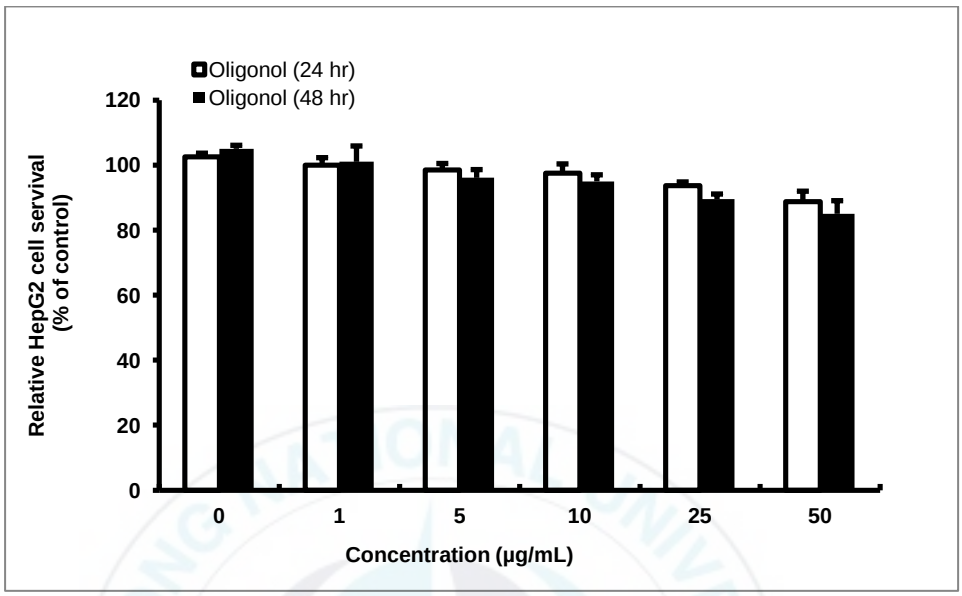

Fig. 14. Oligonol cytotoxicity measurement. HepG2 cells were incubated with various concentrations of oligonol (Ranging from 0 to 50 μg/mL) for 24 or 48 h, and cell viability was measured by MTT assay.

2.2. Establishing an IR cell line.

In order to develop an IR cell line, the HepG2 cells were initially treated with different concentrations of insulin for 36 h (Fig. 15AC). The results indicate that the lowest glucose uptake occurred at an insulin dose of 10^{-6} mol/L (Fig. 15A). HepG2 cells were then exposed to 10^{-6} mol/L insulin for 24, 48 and 72 h (Fig. 15B) and the results demonstrated that insulin-induced glucose uptake was lowest at 24 h (Fig. 15B). Therefore, the IR HepG2 cells used in the present study were established using 10^{-6} mol/L insulin administered to the cells for 24 h. In order to determine the stability of the model, the IR cells were grown in medium without insulin for 24, 48 and 72 h (data not shown) and the results show that the IR cells remained stable for 48 h. Furthermore, the protein expression level of selective insulin concentrations was determined to confirm the insulin resistance by using Western blot method. In Fig. 15C showed that insulin 10^{-6} mol/L decreased the height protein expression level of pAKT in insulin resistance HepG2 cells compared to the control, which is directly related to the insulin signaling pathway. These results suggest that insulin at concentration 10^{-6} mol/L may possess resistance in HepG2 cells.

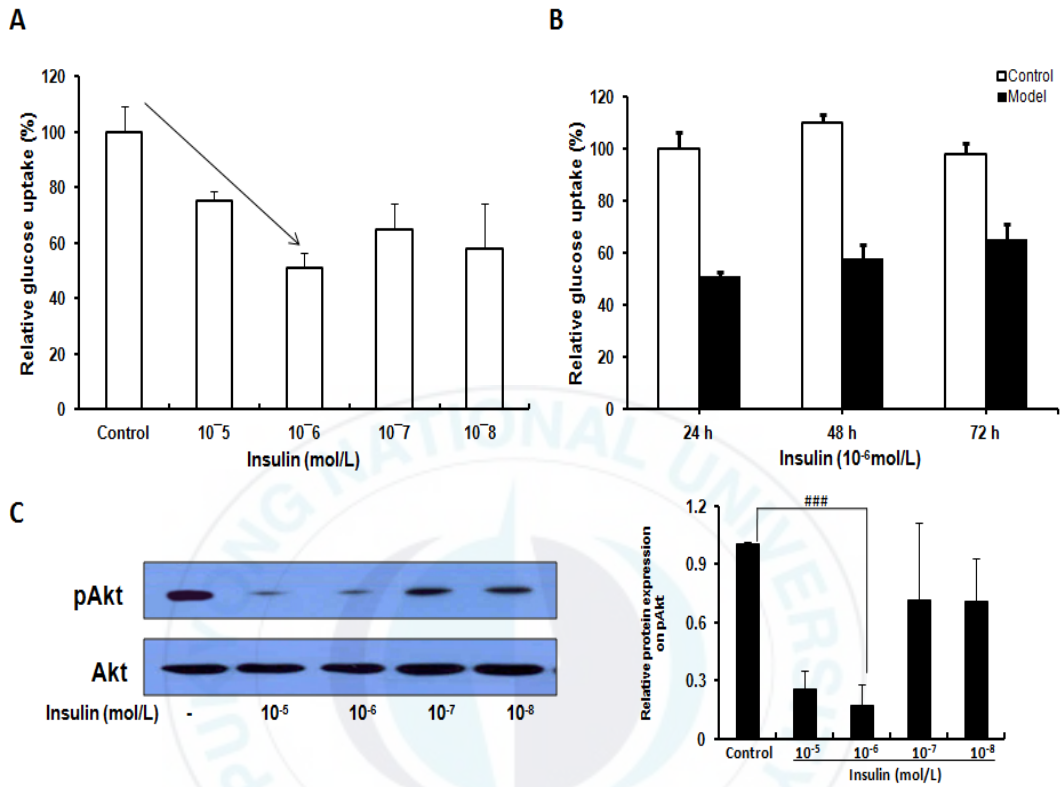

Fig. 15. Establishment of an insulin-resistance HepG2 cell line. (A) Effect of insulin concentration on glucose uptake by HepG2 cells. (B) Effect of insulin treatment time on insulin-induced glucose uptake by HepG2 cells. (C) Effect of insulin concentration on pAkt expression level in insulin-resistance HepG2 cells. Protein band intensities were quantified by densitometric analysis.

2.3. Effect of oligonol on glucose uptake

To determination of the capability of oligonol to increase glucose uptake, the 2-NBDG (a fluorescent glucose analog) uptake assay was performed in insulin-resistant HepG2 cells model. The IR HepG2 cells were pretreated with different nontoxic doses of oligonol (2.5, 5, and 10 μg/mL) for 24 h, according to the reported method (Fig. 16 A). After incubation, 2-NBDG analog was used 20 min to determine the uptake ability of oligonol. It was found that oligonol significantly enhanced the insulin-stimulated uptake in a dose-dependent manner with the significant direction (Fig. 16B), compared to the positive control metformin. Statistical values were presented by the mean ± SD of three independent experiments. ###$p < 0.001$ ensure the significance difference of insulin resistance group from normal control group, *$P < 0.05$, **$P < 0.01$ and ***$P < 0.001$ compared with insulin control group (Fig. 16). In general, glucose uptake is hampered by the insulin resistance condition that is directly correlated to the insulin signaling. These data suggest that oligonol improves insulin sensitivity by the stimulation of glucose uptake in IR HepG2 cells.

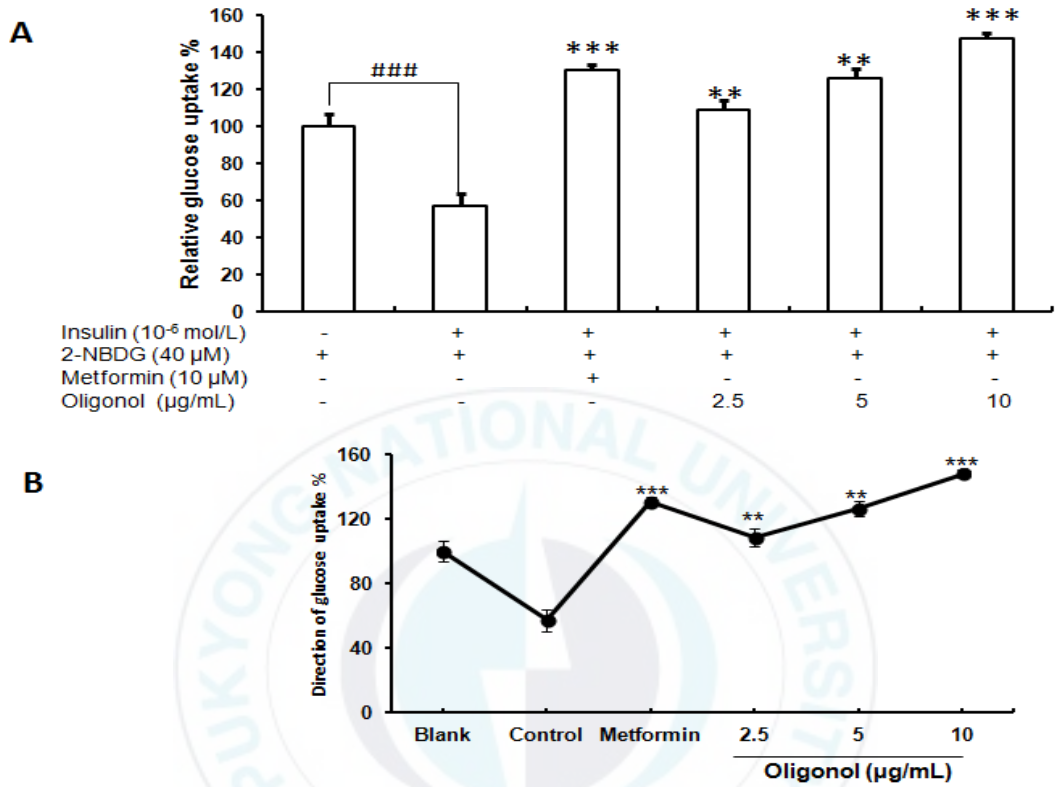

Fig. 16. Effect of oligonol on insulin-stimulated glucose uptake in insulin-resistant HepG2 cells. A glucose uptake assay was performed using the fluorescent D-glucose analogue 2-NBDG. The insulin-resistant HepG2 cells were treated with different concentration oligonol or metformin for 24h, and insulin-stimulated 2-NBDG uptake was measured as described in materials and methods. Relative fluorescence intensity minus background was used for subsequent statistical analyses. Values were the mean ± SD of three independent experiments. *P < 0.05, **P < 0.01 and ***P < 0.001 compared with control.

2.4. Effect of oligonol on PTP1B expression level in insulin-resistant HepG2 cells

PTP1B is an enzyme that is the founding member of the protein tyrosine phosphatase (PTP) family PTP1B negatively regulates insulin signaling and its increased activity and expression are implicated in the pathogenesis of insulin resistance, that is considered a promising potential therapeutic target, in particular for the treatment of type 2 diabetes. Our recent study has been reported that oligonol has potential inhibits PTP1B enzyme activity (Choi et al. 2016). Here, we examined the PTP1B expression in insulin resistance HepG2 cells by Western blot analysis. For determination the PTP1B expression level, insulin resistance HepG2 cells were treated with different concentration (2.5, 5 and 10 μg/mL) of oligonol for 24 hr. Our result showed that PTP1B expression level was significantly decreased more than the normal levels at the dose-dependent manner, where metformin (Positive control drug) decreased PTP1B level similar to the 5 μg/mL of oligonol (Fig. 17). Data were represented means ± standard deviation of triplicate experiments. ###$p < 0.001$ indicates a significance difference of insulin resistance group from the normal control group, which showed, the PTP1B expression level of insulin resistance group was more than

50% compared to a non-insulin resistance group. *P < 0.05, **P < 0.01, and ***P < 0.001 indicate significant difference from the insulin-treated control group of oligonol treated group. This result suggests that oligonol improves insulin sensitivity via decreasing PTP1B expression that stimulates insulin signaling.

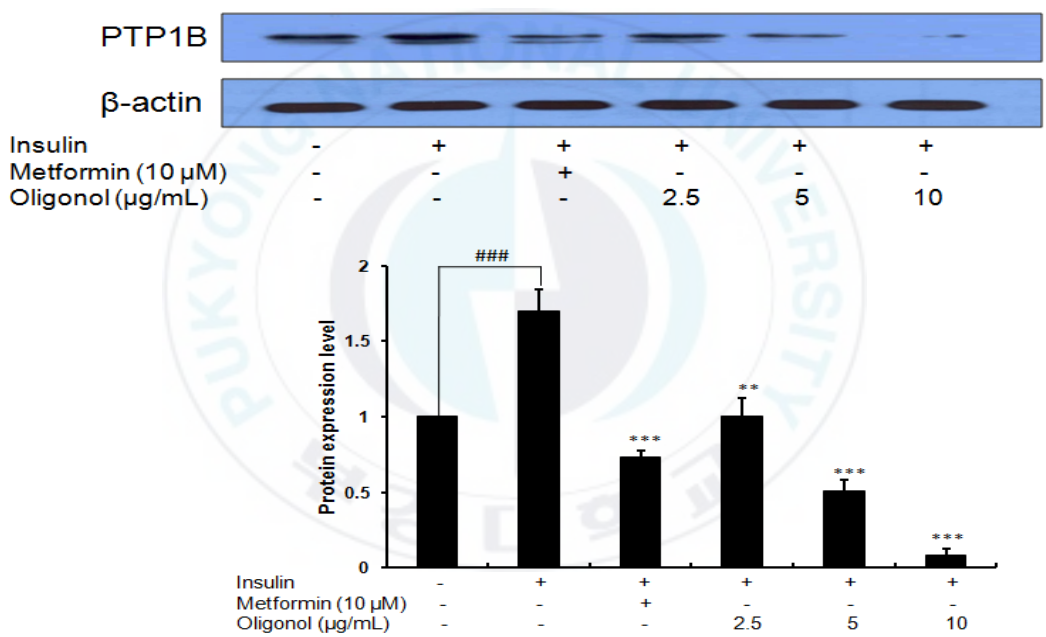

Fig: 17. Inhibitory effects of oligonol on PTP1B expression level in insulin-resistance HepG2 cells. Protein band intensities were quantified by densitometric analysis. Cells were pretreated with the indicated concentration of oligonol and or metformin for 24 h. Data shown represents means ± standard deviation of triplicate experiments. ###p < 0.001 indicates a significance difference from normal control group, *P < 0.05, **P < 0.01, and ***P < 0.001 indicate significant difference from the insulin (10^{-6} mol/L) treated control group.

2.5. Oligonol ameliorates insulin resistance with up-regulated insulin signaling

To determine the insulin sensitive activities of oligonol in insulin resistance condition, we determined the expression levels of various proteins involved in the insulin signaling pathway using Western blotting. We examined the changes in the phosphorylation of insulin receptor substrate-1 (IRS-1) in insulin resistance HepG2 cells. IRS-1 is major substrates of PTP1B; in insulin resistance condition IRS-1 activity is inhibited by the phosphorylation of specific tyrosine or serine residues. First, we confirmed that treatment of oligonol activates IRS-1 by decreasing serine 307 phosphorylation of IRS-1 (Fig. 18). Interestingly, activation of IRS-1 and dephosphorylation of serine 307 was associated with all the 3 concentrations (2.5, 5, and 10 μg/mL) of oligonol at a dose-dependent manner. As shown Fig 5ABC, which indicates a significance difference of normal control group from insulin resistance group, as well as indicates a significant difference of oligonol treated group from insulin control group. Data represent means ± SD of triplicate experiments. ###$p < 0.001$ indicates a significance difference of normal control groups from resistance group, that indicate insulin resistance group causes phosphorylation of IRS-1 at serine 307 residues, *$P < 0.05$, **$P <$

0.01, and ***$P < 0.001$ indicate oligonol significantly reduced the serine 307 phosphorylation in a dose-dependent manner compared to the insulin resistance groups (Fig. 5AC). Furthermore, we then explored whether the substrates and the downstream signals PI3K-Akt were affected by oligonol in insulin-resistance HepG2 cells. As shown in Fig. 19CB, oligonol dose-dependently increased the expressions of p-PI3K and p-Akt, while did not affect the expression levels of the PI3K and total Akt (Fig. 5AED), which stimulates insulin sensitivity as well as regulates intercellular glycogen synthesis by enhancing the glucose uptake. Statistical data shown represents means ± SD of triplicate experiments.

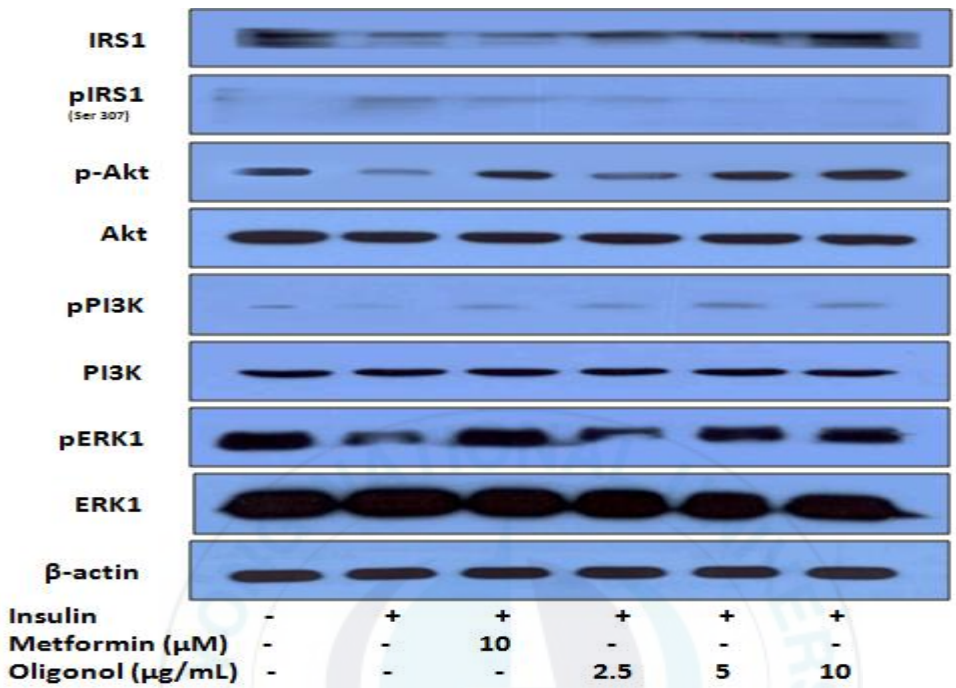

Fig: 18. Effect of oligonol on the relative protein expression of total and phosphorylated IRS-1/AKt/PI3K/ERK1 pathway in insulin-resistant HepG2 cells. The expression levels were determined by Western blot analysis. Equal protein loading was ensured and normalized against β-actin levels. The results were similar from three independent experiments. Protein band intensities were quantified by densitometric analysis by using CS analyzer eng software. Values are expressed as mean ± standard deviations of three independent experiments.

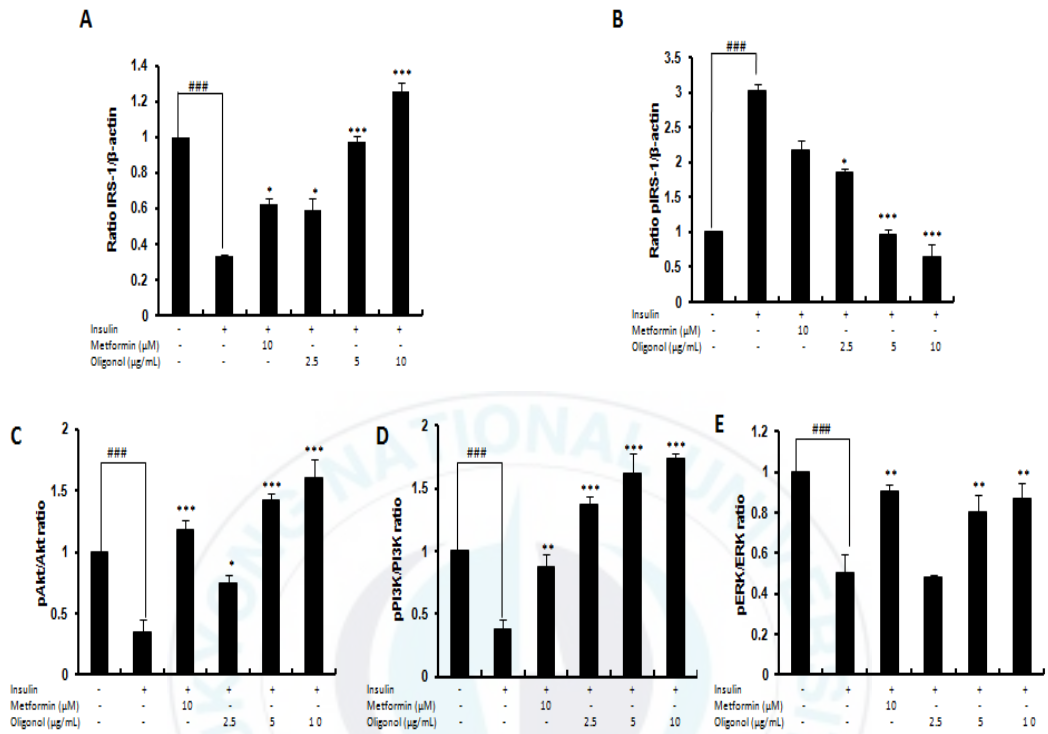

Fig: 19. Densitometric analysis of oligonol on the levels of phosphorylated and total insulin receptor substrate 1 (IRS1)/phosphatidylinositol-3-kinase (PI3K)/Akt/extracellular regulated kinase1 (ERK1) in insulin-resistant HepG2 cells by using CS analyzer eng software. Values are expressed as ratios of IRS-1/ β-actin (A), pIRS-1 (Ser 307)/β-actin (B), p-Akt/Akt (C), pPI3K/PI3K (D), and pERK1/ERK1 (E). Mean ± standard deviations of three independent experiments. **P* < 0.05, ***P* < 0.01, and ****P* < 0.001 were considered significant compared with control.

2.5.1. Effects of oligonol on the phosphorylated and total levels of ERK1 in insulin resistant HepG2 cells

To test the effects of oligonol on levels of ERK1, insulin-resistant HepG2 cells were incubated with different concentrations of oligonol (2.5, 5 and 10 μg/mL), and the phosphorylated and total ERK1 were evaluated in cell lysates by Western blotting (Fig. 18, and 19D). As shown in Fig.19D the treatment of insulin-resistant cells with any of the three concentrations of oligonol with or without metformin increased the phosphorylation level of ERK1 in a dose-dependent manner. Metformin was used in these experiments as a positive control. These findings indicate that oligonol increased the expression of IR levels, and activated the downstream PI3K/Akt signaling pathway, as well as ERK1 and therefore, enhanced insulin sensitivity in insulin-resistant HepG2 cells.

2.5.2. Oligonol prevents Caspass-3 activation

To test whether insulin resistance cell death is correlated with cell apoptosis, HepG2 cells were incubated with different concentration of oligonol, and the caspas-3 activation was determined by the Western blot method. In Fig. 20 showed that oligonol dose-dependently inhibits the activation of caspass-3

activation. According to our result, oligonol has a preventive activity against caspass-3 activation.

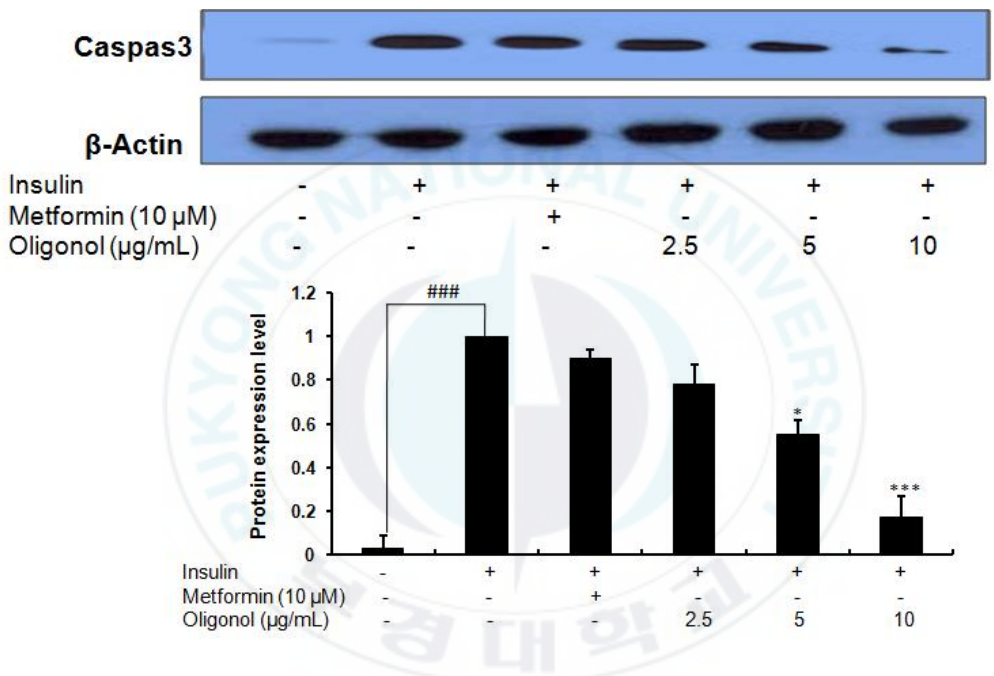

Fig. 20. Inhibitory effects of oligonol on caspase-3 activation in insulin-resistance HepG2 cells. Protein band intensities were quantified by densitometric analysis, which was insulin control, set to 1. Cells were pretreated with the indicated concentration of oligonol and or metformin for 24 h. Data shown represents means ± standard deviation of triplicate experiments. ###$p < 0.001$ indicates a significance difference from normal control group, *$P < 0.05$, and ***$P < 0.001$ indicate significant difference from the insulin control group.

2.5.3. Inhibitory effects of oligonol on NF-κB protein expression

The protein level of transcription factor NF-κB was determined by Western blot method in insulin resistance HepG2 cells. NF-κB expressed in the cytoplasm of all cell types, where a family of regulatory proteins controlled its activity. Actually, the activation of NF-κB depended on the detection of its translocation into the cell nuclei. Western blotting of NF-κB p65 protein in insulin resistance HepG2 cells indicates that insulin resistance induced by high concentration of insulin enhances the nuclear NF-κB in cells. As shown in Fig. 21 demonstrated that oligonol significantly inhibited the nuclear NF-κB on the insulin resistance HepG2 cells. The relative level of NF-κB p65 expression compared with the β-actin and quantified by CS analyzer. Our result demonstrated that insulin resistance HepG2 cells had increased the level of NF-κB p65 protein expression compared with the normal control group. Moreover, oligonol significantly reduced the expression of NF-κB p65 proteins in insulin resistance HepG2 cells in a dose-dependent manner compared to the normal and insulin resistance group. Data were represented means ± standard deviation of triplicate experiments. ###$p < 0.001$ compared with the normal control and insulin resistance group, *$P <$

0.05, and ***P < 0.001 indicate significant difference from the insulin control group (Fig. 21).

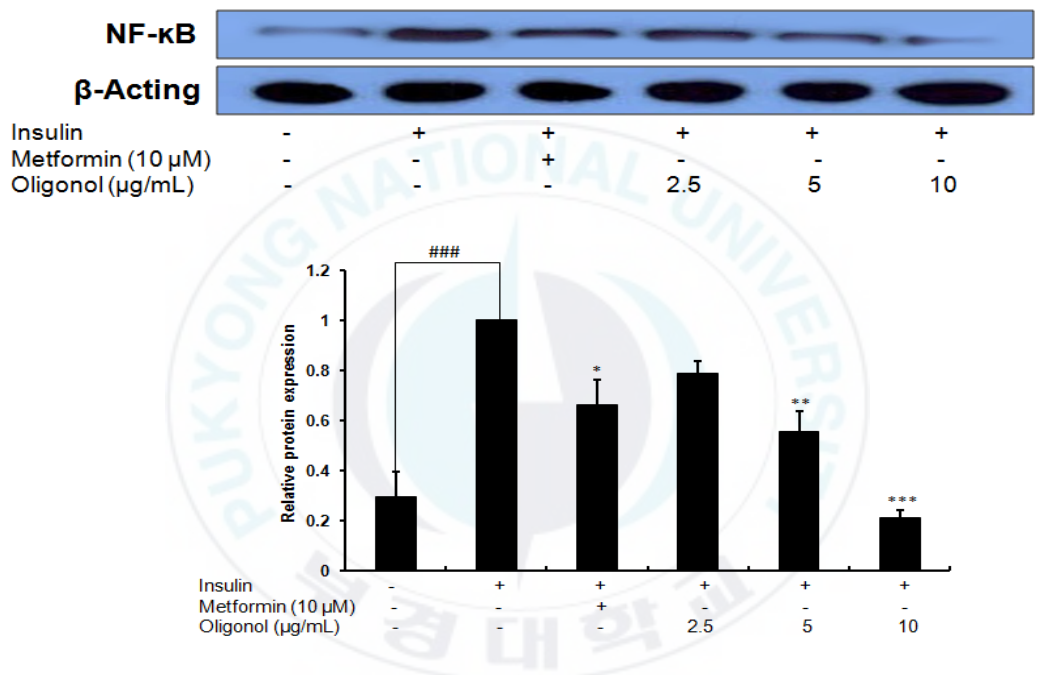

Fig.21. Effects of oligonol on NF-κB inhibition in insulin-resistance HepG2 cells. Protein band intensities were quantified by densitometric analysis, which was insulin control, set to 1. Cells were pretreated with the indicated concentration of oligonol and or metformin for 24 h. Data shown represents means ± standard deviation of triplicate experiments. ###p < 0.001 indicates a significance difference from normal control group, *P < 0.05, and ***P < 0.001 indicate significant difference from the insulin control group.

2.6. Hepatoprotective properties of oligonol

2.6.1 Hepatoprotective property of oligonol in *t*-BHP treated HEpG2 cells

To determine the hepatoprotective effects of oligonol on *t*-BHP-treated HepG2 cells, cells were pretreated with the different concentrations of oligonol (2.5, 5, 10 µg/mL) for 24 h. After treatment of oligonol cells were treated with 200 µM of *t*-BHP followed by 2 h incubation in 37^0C condition. As shown in Fig. 22, treatment with oligonol increased the cell viability of *t*-BHP treated HepG2 cells in a dose-dependent manner. Interestingly, oligonol at concentration 5 µg/mL increased the cell viability, similar to achieved upon treatment with 10 µg/mL of silymarin, a well-reported hepatoprotective drug. While oligonol treated at concentration 10 µg/mL, cell viability percentage was more than the silymarin (Fig. 22). According to the results, it is clear that pretreatment of HepG2 cells with oligonol significantly protected HepG2 cells against *t*-BHP induced cytotoxicity.

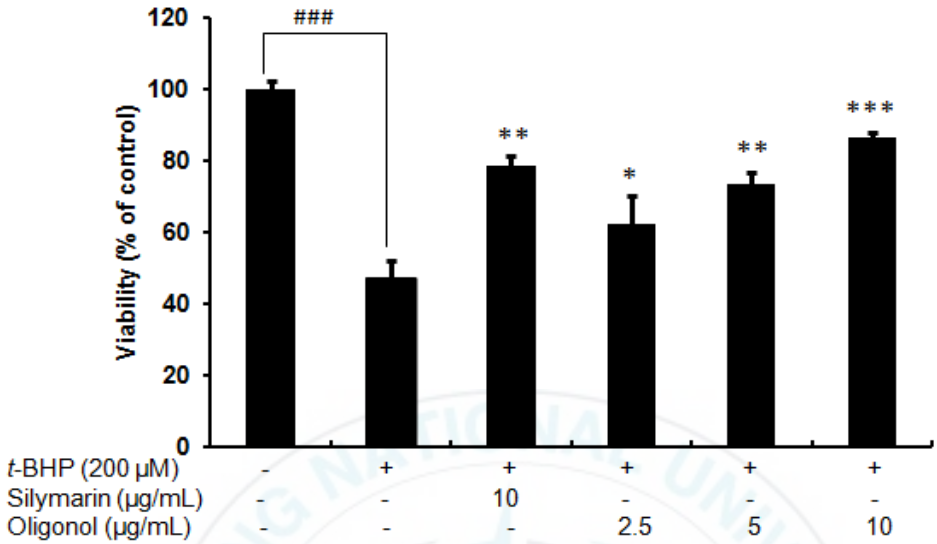

Fig. 22. Effect of oligonol on HepG2 cell damage induced by *t*-BHP. Cells were pretreated with the indicated concentration for 24 h followed by *t*-BHP (200μM for 2 h). Cell viability was assessed using MTT assay. Data shown represents means ± standard deviation of triplicate experiments. ###$p < 0.001$ indicates a significance difference from normal control group, *$P < 0.05$, **$P < 0.01$, and ***$P < 0.001$ indicate significant difference from the *t*-BHP treated control group.

2.6.2 Effect of oligonol on the levels of intracellular ROS in *t*-BHP treated HepG2 cells

For the determination whether the observed cytoprotective effect of oligonol attributed towards the reduction of oxidative stress, we next determined the effects of oligonol on ROS generation in cellular level (HepG2 cells) exposed by *t*-BHP (200 μM). Exposures of *t*-BHP (200 μM), that generates intracellular ROS level was estimated using the ROS-sensitive fluorescence indicator DCFH-DA. *t*-BHP increased the generation of ROS in HePG2 cells to the levels of about 100%. Therefore, the effects of oligonol on ROS generation in *t*-BHP treated HepG2 cells in shown in Fig. 11. Pretreatment of different concentration of oligonol significantly inhibits the generation of intracellular ROS in HepG2 cells at concentration-dependent manner. Moreover, at concentrations exceeding 10 μg/mL of oligonol almost totally inhibited the generation of ROS in *t*-BHP-treated HepG2 cells (Fig. 23). Trolox was used as positive control.

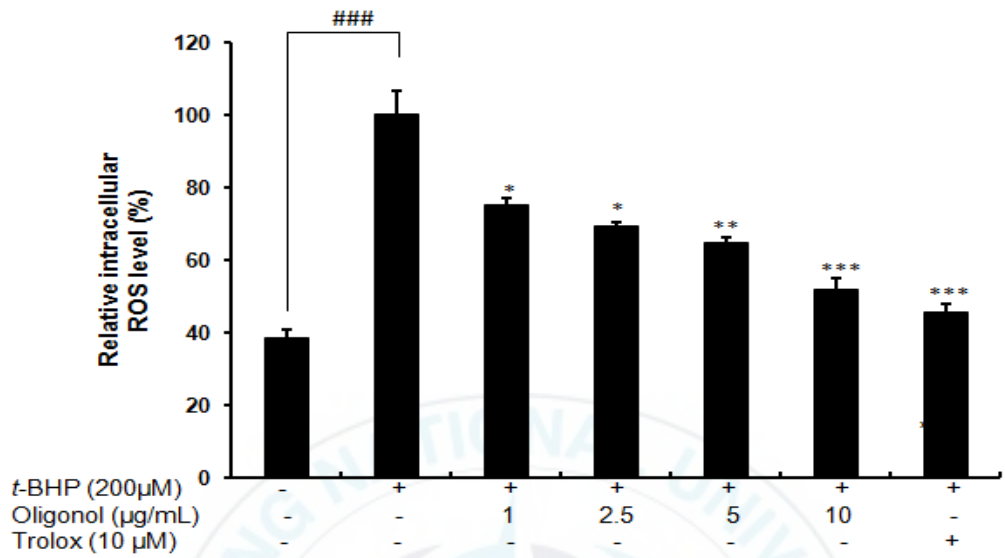

Fig. 23. Effects of oligonol on *t*-BHP induced ROS generation in HepG2 cell. Values are expressed as the mean ± SD of triplicate experiments. ###$p < 0.001$ indicates a significance difference from the *t*-BHP untreated control group, *$P < 0.05$, **$P < 0.01$, and ***$P < 0.001$ indicate significant difference from the *t*-BHP treated control group.

2.6.3. Total ROS scavenging activities of oligonol.

In order to identify the ROS scavenging agents from a natural source, we selected oligonol due to its various biological activities. The results are presented in Table 4. As shown in Table 4 and fig. 24B, oligonol exhibited potent scavenging activities on total ROS within the range of 47.18 ± 2.11% to 87.85 ± 0.63 % at concentration 1.6, 8, 40 μg/mL in a dose-dependent manner with the IC_{50} value of 2.30 ± 0.32 μg/mL. Trolox was used as positive control (IC_{50}= 4.31±0.19).

2.6.4. $ONOO^-$ scavenging activity of oligonol

$ONOO^-$ scavengers play an important role in various pharmacological effects and physiological condition, such as diabetics' mellitus, Alzheimer's disease, and oxidative stress in various organs. Generally, $ONOO^-$ is generated in the body by cellular metabolism that is responsible for metabolic disorders. So, $ONOO^-$ scavengers from natural source observed in vitro will be a great target to ameliorate several oxidative stress related disease, including DM, AD, aging, and inflammation. As shown in Table 4, and Fig 24A, oligonol exhibited significant $ONOO^-$ scavenging activity with IC_{50} values of 17.98 ± 0.76 μg/mL, compared to

the positive control L-penicillamine with IC_{50} values of 5.18 ± 0.39 μg/mL. These findings demonstrated that oligonol is the principle constituents for the antioxidant activities, which may be directly related to the anti-DM, anti-AD, as well as hepatoprotective activity.

Table 4. $ONOO^-$ and total ROS scavenging activity of oligonol

Name of compounds	IC_{50} (μg/mL)[a]	
	$ONOO^-$ scavenging activity	Total ROS scavenging activity
Oligonol	17.98 ± 0.76	2.30 ± 0.32
Penicillamine[b]	5.18 ± 0.39	
Trolox[c]		4.31 ± 0.19

[a] 50% inhibitions are expressed as the mean ± SEM of double experiments.
[b,c]Positive control.

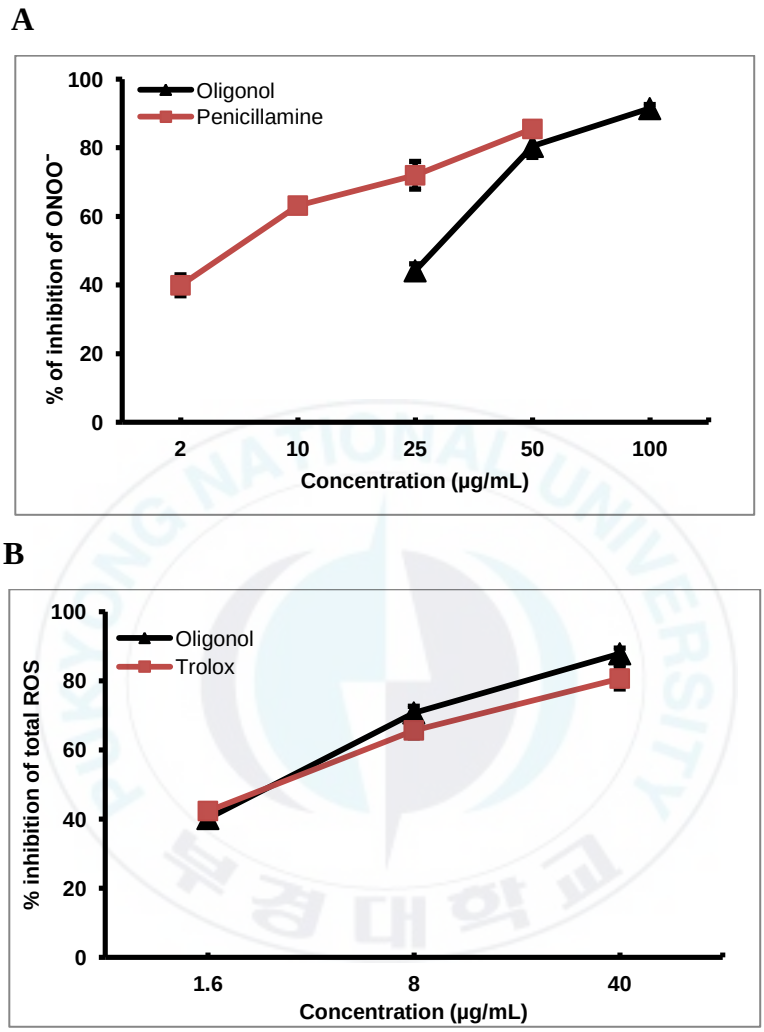

Fig. 24. Concentration-dependent scavenging activity of oligonol and penicillamine on $ONOO^-$(A) and oligonol and ursolic acid on total ROS (B) was analyzed in the presence of various sample concentrations, as follows: 100, 50, 25, 10, 2 μg/mL for $ONOO^-$ and 40, 8, 1.6 μg/mL for ROS inhibition respectively.

2.7. Molecular docking simulation studies

We next used molecular docking studies to obtain accurate predictions of protein-ligand interaction geometries for the constituents of oligonol and PTP1B. Compound 23 was used as a control ligand for validation in Autodock 4.2. The docking scores of the selected constituents with interacting residues as well as the number of hydrogen bonds formed between interacting residues and Vander Waals bond interacting residues are shown in Table 5. We found that the activity of the selected constituents of oligonol against PTP1B correlated with the binding energy and number of hydrogen bonds formed in the active site (Fig. 25-29).

2.7.1. Docking of the oligonol catechin on PTP1B enzyme

The binding affinity of catechin towards PTP1B was –8.24 kcal/mol, and GLY209, HIS208, SER80, LYS73, VAL211, PRO210, SER205, PRO206, GLN78, LEU204, ARG79, and SER203 were identified as interacting residues. Catechin bound with PTP1B by forming 6 hydrogen bonds as shown in Fig. 25A, 26A and Table 5. Specifically, catechin-PTP1B binding involved the formation of three hydrogen bonds with the SER80 residue, interacting oxygen and nitrogen atom group with the hydroxyl group of catechin. Similarly, we found that the Gly209 and His208 residues forms individual hydrogen bonds with the same

hydroxyl group at position 13 of catechin group no 3 , while the lys73 residue was formed a single hydrogen bond with the C_{19} position of catechin (Fig. 26A). In addition to the residues described above, the residues SER205, PRO206, GLN78, LEU204, ARG79, and SER203 were found to form Van der Waals interactions, thereby strengthening the protein-ligand interaction between PTP1B and catechin.

2.7.2. Docking of the oligonol epicatechin on PTP1B enzyme

As shown in Fig. 25B and Table 5, the constituents of oligonol (Epicatechin) formed seven hydrogen bond interactions with GLY209, HIS208, SER80, LYS73, and SER205 residues and had a binding affinity of –8.27 kcal/mol for PTP1B. In addition, one of the hydroxyl groups of epicatechin(C-13) was found to interact with the residues (GLY209, SER205, and HIS208) of PTP1B by forming three hydrogen bond interactions. In addition, the SER80 residue interacted with epicatechin by forming three hydrogen bond at position (C-18, C-19, and C-11). Interestingly, the nitrogen atom of LYS73 residue was found to form a hydrogen bond with the hydroxyl group of epicatechin (C-19). In addition, several hydrogen bond interactions appeared to be involved between oxygen and nitrogen atoms of PTP1B residues and the hydroxyl groups of

epicatechin. We also noted Vander Waals interaction interactions between epicatechin with SER203, VAL211, PRO206, GLN78, ARG79, LEU204, and PRO210 that further stabilized the protein-ligand interaction (Fig. 26B).

2.7.3. Docking of the oligonol Epigallocatechin on PTP1B enzyme

The SER80 residues of PTP1B were found to form three hydrogen bonds with the epigallocatechin on position C-20, C-13, C-19, as well as His208 and Gly was formed single hydrogen bond with C-14 position of epigallocatechin, which had a binding affinity of –7.85 kcal/mol (Fig. 25C, 26C and Table 5), respectively. Molecular docking studies also revealed significant interactions between oxygen atoms of PTP1B with hydrogen atoms present in the epigallocatechin. Whereas, LEU204, ARG79, SER205, PRO206, GLN78, LYS73, PRO210, SER203, and VAL211 were identified as strengthening the binding between epigallocatechin and PTP1B through Van der Waals interactions.

2.7.4. Docking of the oligonol Epigallocatechin gallate on PTP1B enzyme

Epigallocatechin gallate one of the constituents of oligonol was found to interact with PTP1B by forming six hydrogen bonds and had a binding affinity of –6.91 kcal/mol (Fig. 25D, 26D and Table 5), respectively. Similar to the epicatechin, the nitrogen atom of LYS73 residue was involved in interaction with two hydroxyl group of epigallocatechin gallate (C-24, C-26). In addition, the ARG79 and GLN 78 residues were separately involved in two hydrogen bonds interaction with the same hydroxyl group of epigallocatechin gallate (C-23). The GLN102 residue of PTP1B formed a single hydrogen bond. Strong hydrophobic Van der Waals interactions between the epigallocatechin gallate and the PTP1B residues LEU204, PRE206, GLY209, HIS208, PRO210, and LEU71 served to strengthen the protein-ligand interaction.

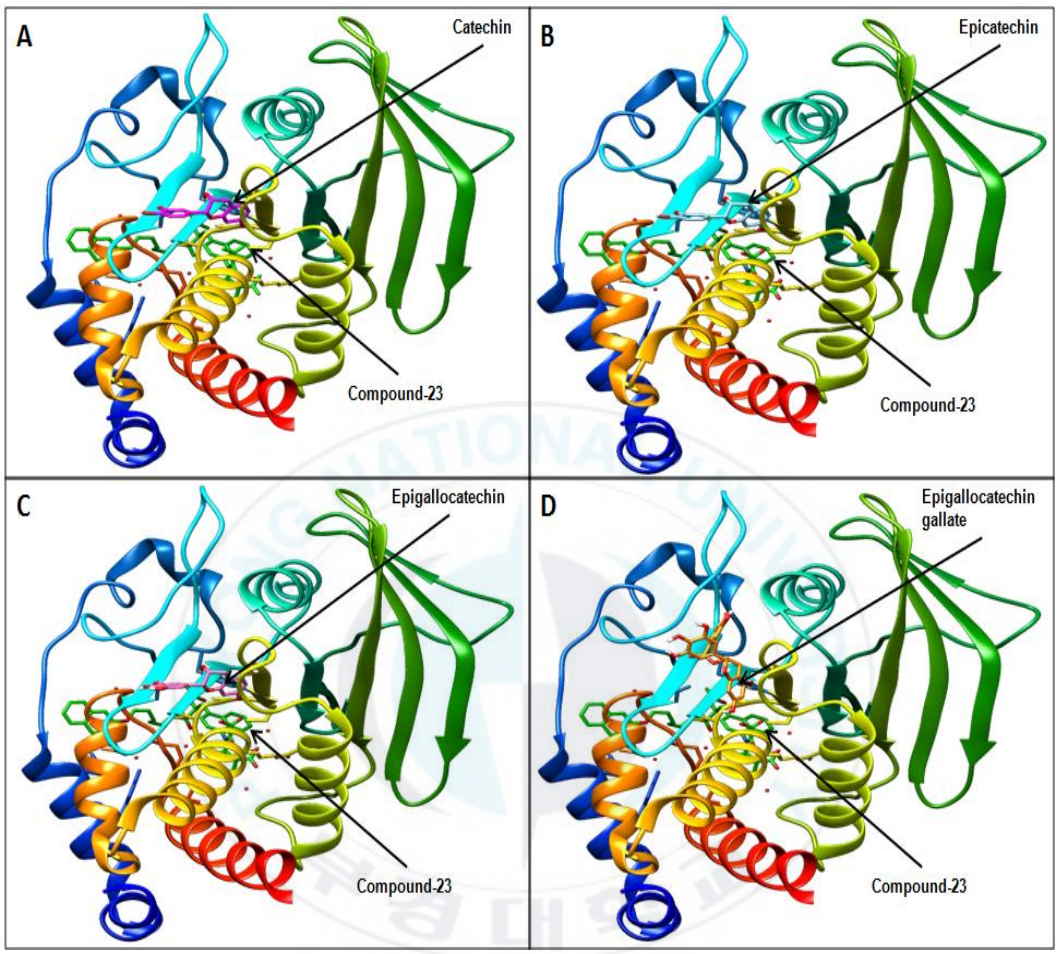

Fig. 25. 3D crystal structure of molecular docking simulation of oligonol constituent's, catechin, epicatechin, epigallocatechin, and epigallocatechin gallate against PIP1B. Compound 23 used as a standard control.

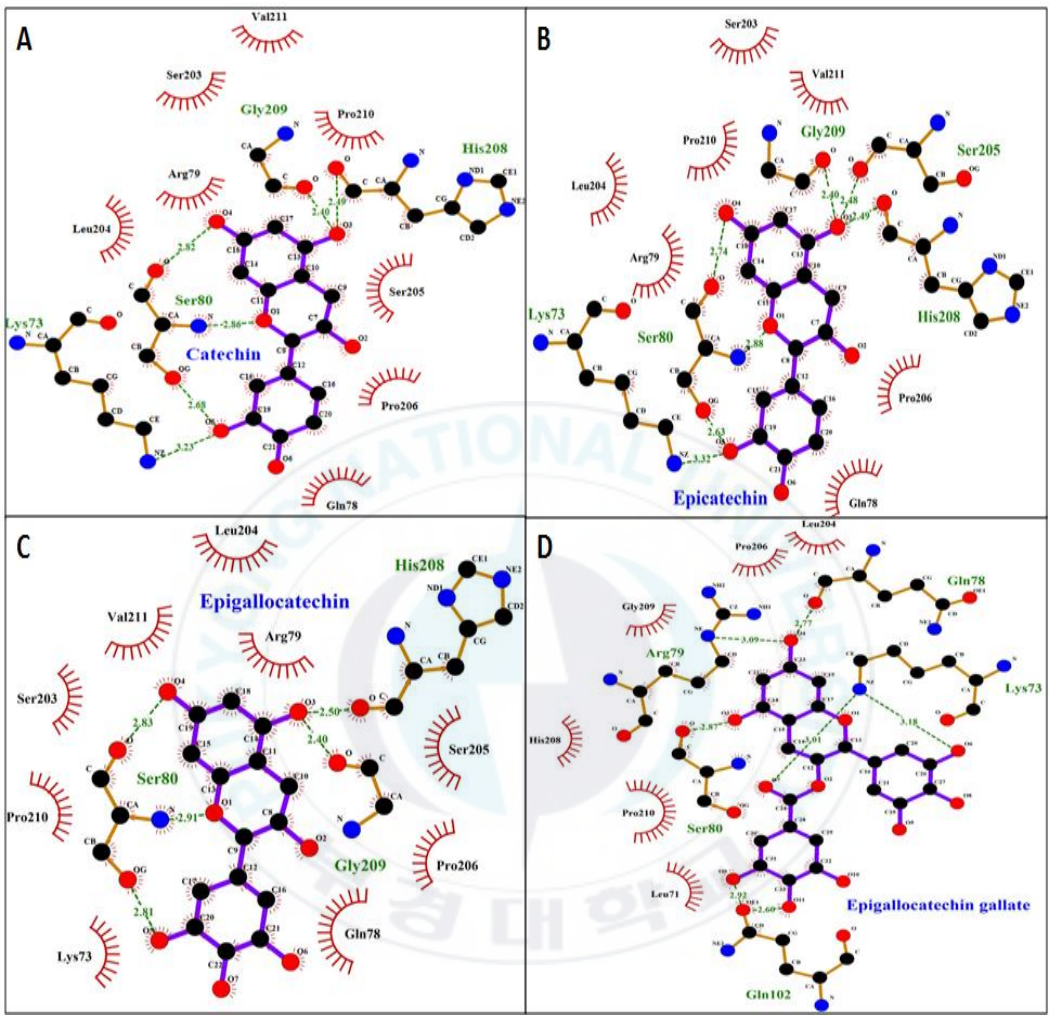

Fig. 26. 2D crystal structure of molecular docking simulation of oligonol constituents catechin, epicatechin, epigallocatechin, epigallocatechin gallate against PIP1B. Compound 23 used as a standard control.

2.7.5. Docking of the oligonol Procyanidin A1 on PTP1B enzyme

Docking interactions between the Procyanidin A1 on PTP1B enzyme are shown in Fig. 27A, 28A. A total of eight hydrogen bonds were observed between procyanidin A1 and the residues ASP137 forming three, ILE134 forms two, and LYS131, GLN127 with LYS128 forming one hydrogen bonds by interacting with the hydroxyl group procyanidin A1. The binding affinity of procyanidin with PTP1B was –6.85 kcal/mol as shown in Table 5. The hydrophobic residues GLY93, PRO162, GLN123, MET133, GLU136, and PHE135 were found to strengthen the interactions between PTP1B and procyanidin through Vander Waals interactions.

2.7.6. Docking of the oligonol Procyanidin A2 on PTP1B enzyme

Procyanidin A2 was found to form 8 hydrogen bonds with PTP1B and had a binding affinity of –8.38 kcal/mol as shown in Fig. 27B, 28B and Table 5, respectively. Similar to the Procyanidin A1 ASP137 forming three, ILE134 forming two, and LYS131, GLN127 with LYS128 forming one hydrogen bonds by interacting with the hydroxyl group procyanidin A2, whereas, a nitrogen atom and an oxygen atom of ASP137 residue formed hydrogen bond at the same

hydroxyl group of procyanidin A2 at position C-38. The GLU136, PHE135, MET133, PRO126, GLN123, and GLY93 residues were identified as being important for the binding of procyanidin A2 and PTP1B through Van der Waals interactions.

2.7.7. Docking of the oligonol procyanidin B1 on PTP1B enzyme

As shown in Fig. 27C, 28C and Table 5, procyanidin B1 formed 5 hydrogen bond interactions with LYS73, SER80, GLN102, and LEU204 residues and had a binding affinity of –6.56 kcal/mol for PTP1B. In addition, one of the hydroxyl groups of procyanidin (C-14) was found to interact with the residues (LYS73, and SER80) of PTP1B by forming three hydrogen bond interactions. In addition, the GLN102 residue interacted with procyanidin B1 by forming two hydrogen bond at position (C-40, C-42). The LEU204 residue was found to form a hydrogen bond with the hydroxyl group of epicatechin (C-33). We also noted Vander Waals interaction interactions between procyanidin B1with GLU75, PRO206, GLY209, HIS208, PRO210, ARG79, GLN78, and MET74 that further stabilized the protein-ligand interaction.

2.7.8. Docking of the oligonol Procyanidin B2 on PTP1B enzyme

Docking interactions between the Procyanidin B2 on PTP1B enzyme are shown in Fig. 27D, 28D. A total of five hydrogen bonds were observed between procyanidin B2 and the residues SER80 forming two, GLU207, VAL211, and SER203 forming one hydrogen bonds by interacting with the hydroxyl group procyanidin B2. The binding affinity of procyanidin B2 with PTP1B was –7.27 kcal/mol as shown in Table 5. The hydrophobic residues LYS103, HIS208, GLY209, PRO210, SER205, ARG79, LEU204, PRO206, GLN78, and LYS73 were found to strengthen the interactions between PTP1B and procyanidin through Vander Waals interactions.

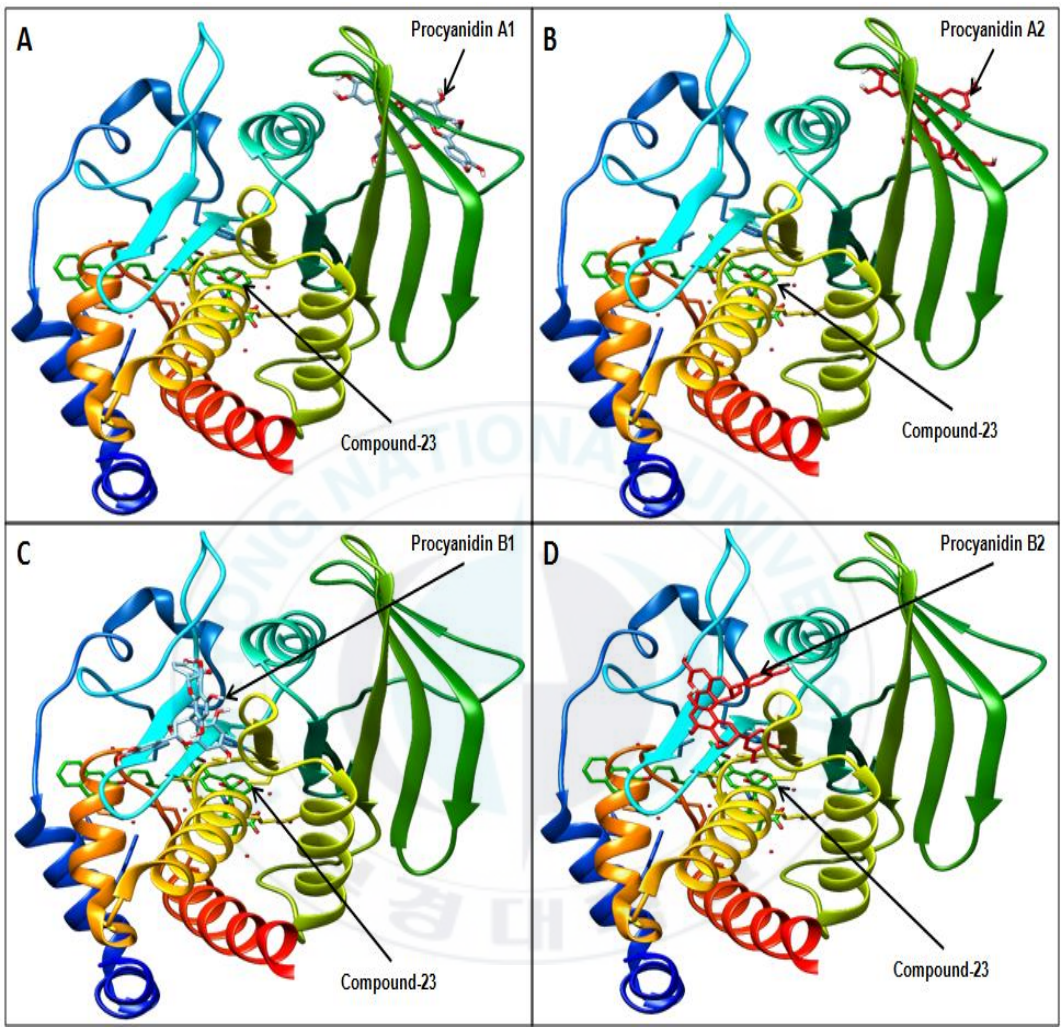

Fig. 27. 3D crystal structure of molecular docking simulation of oligonol constituents procyanidin A1, procyanidin A2, procyanidin B1, procyanidin B2, against PIP1B. Compound 23 used as a standard control.

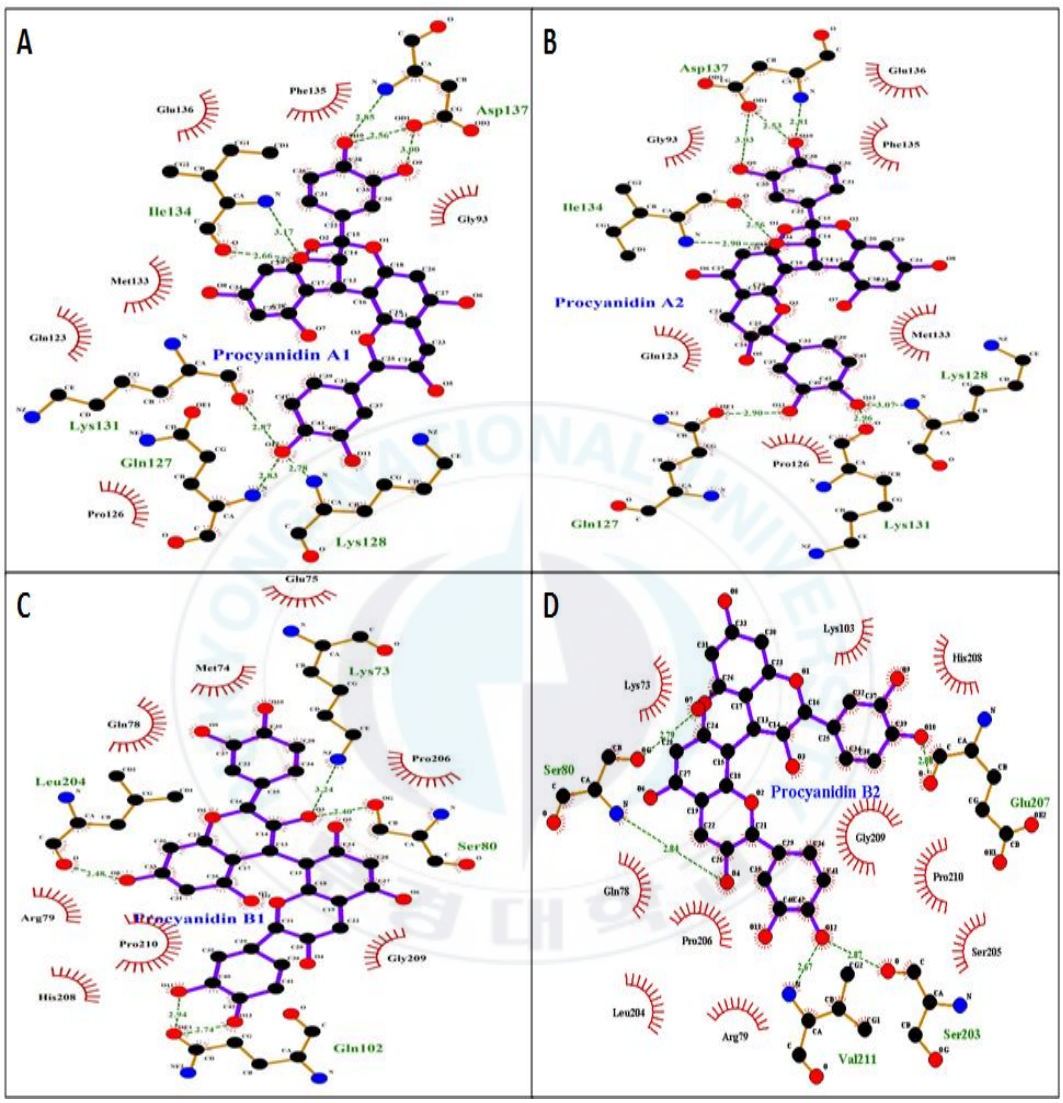

Fig. 28. 2D crystal structure of molecular docking simulation of oligonol constituent's procyanidin A1, procyanidin A2, procyanidin B1, procyanidin B2 against PIP1B. Compound 23 used as a standard control.

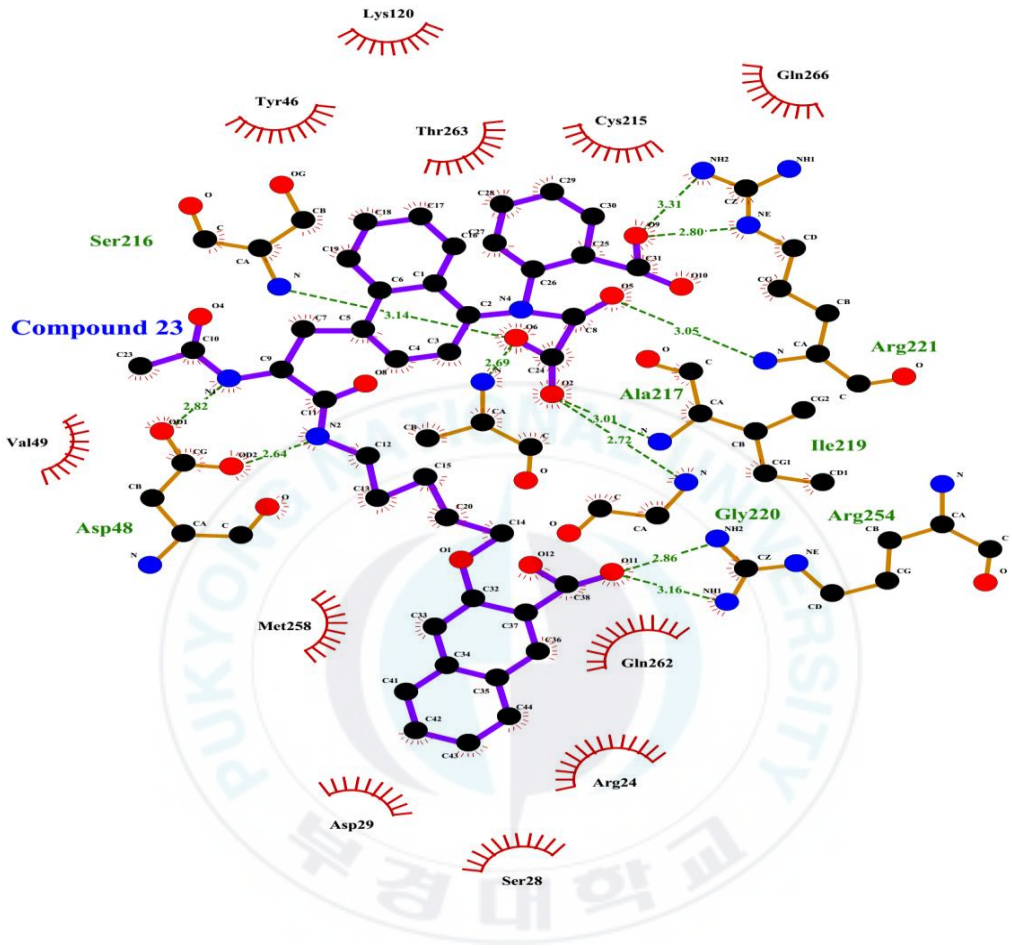

Fig. 29. 2D crystal structure of molecular docking simulation of compound 23 used as a standard control.

Table 5. Molecular interaction of PTP1B active site with known inhibitor compound 23, and constituents of oligonol.

Compound	Binding energy (kcal/mol)[a]	No. of H-bond[b]	H-bond interacting residues[c]	Van der Waals bond interacting residues[d]
Compound 23	-10.18	11	ARG221, SER216, ASP48, GLY220, ARG254, ALA217, ILE219.	TYR46, LYS120, THR263, CYS215, GLN266, GLN262, ARG24, SER28, ASP29, MET258, VAL49
Catechin	-8.24	6	GLY209, HIS208, SER80, LYS73	VAL211, PRO210, SER205, PRO206, GLN78, LEU204, ARG79, SER203.
Epicatechin	-8.27	7	GLY209, HIS208, SER80, LYS73, SER205,	SER203, VAL211, PRO206, GLN78, ARG79, LEU204, PRO210.
Epigallocatechin	-7.85	5	HIS208, SER80, GLY209	LEU204, ARG79, SER205, PRO206, GLN78, LYS73, PRO210, SER203, VAL211
Epigallocatechin gallate	-6.91	6	ARG79, GLN78, LYS73, GLN102, SER80,	LEU204, PRE206, GLY209, HIS208, PRO210, LEU71
Procyanidin A1	-6.85	8	ASP137, LYS128, GLN127, LYS131, LLE134	GLY93, PRO162, GLN123, MET133, GLU136, PHE135
Procyanidin A2	-8.38	8	ASP137, ILE134, GLN127, LYS131, LYS128	GLU136, PHE135, MET133, PRO126, GLN123, GLY93
Procyanidin B1	-6.56	5	LYS73, SER80, GLN102, LEU204	GLU75, PRO206, GLY209, HIS208, PRO210, ARG79, GLN78, MET74.
Procyanidin B2	-7.27	5	GLU207, SER203, VAL211, SER80	LYS103, HIS208, GLY209, PRO210, SER205, ARG79, LEU204, PRO206, GLN78, LYS73.

[a] Binding energy, which indicates binding affinity and capacity for the active site of PTP1B enzyme.

[b,c,d] The number of hydrogen bonds, and all amino acid residues from the enzyme-inhibitor complex were determined by Autodock 4.2 program.

2.8. Discussion

Insulin resistance is a major pathophysiological condition of DM, is usually accompanied by hyperinsulinemia as a result of relative hyperglycemia to override diminished insulin action. The pathology of hyperinsulinemia induced IR is associated with hyper-Ser/Thr phosphorylation of IRS1 and IRS2 that impairs their interaction with the cytoplasmic domain of insulin receptors, which abolished the propagation of normal insulin signaling. On the other hand, stimulation of glucose uptake and enhancement of insulin signaling are important anti-hyperglycemia mechanisms in hepatocytes (Shen et al. 2008), which is responsible for hepatic glycogen synthesis (Newgard et al. 2000). Impaired glucose uptake leads to high circulating glucose levels, therefore, the strategy to the treatment of T2DM is to stimulate glucose uptake in skeletal muscle, liver, and adipose tissue that consume most plasma glucose. Pathophysiology of DM is not only about an insulin-glucose axis, but oxidative stress and inflammation are also a major cause of T2DM. Although different groups of antidiabetic agents have been used in the clinic, it is difficult to meet all patients' needs. Recent year, the development of new insulin sensitizing agents is in great demand. Because insulin resistance is the main causes of T2DM, ameliorating insulin resistance has

been considered as a major clinical strategy to mitigate metabolic control in T2DM (Tahrani et al. 2011). On the other hand, PTP1B involved in the insulin resistance pathway as a main negative regulator of insulin signaling (Panzhinskiy et al. 2013; Tiganis 2013). There are several researchers have been demonstrated that the levels of PTP1B expression in muscle and adipose tissues of humans are directly and or indirectly related to insulin resistance states (Ahmad et al. 1997; Cheung et al. 1999; Stull et al. 2012). Recent studies have reported that PTP1B inhibitor increased the tyrosine phosphorylation of IR, and activated the downstream molecules of insulin signaling such as IRS-1, Akt, and ERK1 (Maeda et al. 2014; Takada et al. 2012), because of that IRβ and IRS-1 are two major substrates of PTP1B. In addition, the reduction in PTP1B expression and activity, enhance the insulin signaling pathway and to improve insulin sensitivity (Elchebly et al. 1999; Gum et al. 2003; Klaman et al. 2000). Therefore, the inhibitors of PTP1B would be potential antidiabetic agents, which effects by enhancing insulin sensitivity in T2DM (Panzhinskiy et al. 2013; Popov 2011). In a continuing search for new PTP1B inhibitors and insulin sensitizing agents from a natural source, we have found a new agent, named oligonol. Recently, the molecular mechanisms of oligonol against diabetes attracted much attention.

Several pharmacological studies have found that oligonol could improve insulin sensitivity may help to protect against DM-related complications and attenuate antioxidant, anti-inflammatory and anti-aging actions than general polyphenol (Nishioka et al. 2006; Tomobe et al. 2007; Kundu et al. 2008; Sakurai et al. 2008). Our recent study also demonstrated that oligonol has potential PTP1B and α-glucosidase inhibitory activities (Choi et al. 2016), till now the actual anti-DM mechanism of oligonol remains unknown.

In the present study, we investigated the underlying mechanisms of the effects of oligonol against insulin resistance *in vitro*, as well as the effects of oligonol against oxidative stress, induced by *t*-BHP in HepG2 cells. We also investigate the specific binding affinity of the constituents of oligonol on PTP1B using computational docking analysis, whereas Autodock 4.2, Chimera, Lig Plus, Discovery Studio and others related software were used. For the investigation of the glucose uptake ability, insulin resistance in HepG2 cells was induced by the incubation with insulin (10^{-6} mol/L, for 24 h), as judged nearby a 60% decrease in glucose uptake (Fig. 15AB). Western blot method was also used to confirm the insulin resistance condition in HepG2 cells model (Fig. 15C). This was improved by prior incubation of HepG2 cells with oligonol for 24 h. Our results also

showed that oligonol increased the glucose uptake in a dose-dependent manner (Fig. 16). Glucose uptake assay was performed using the fluorescent D-glucose analogue 2-NBDG. The insulin-resistant HepG2 cells were treated with different concentration oligonol (2.5, 5, and 10 μg/mL) or metformin (10 μM) for 24h (Fig. 16A), and insulin-stimulated glucose uptake was measured as described in materials and methods. Values were the mean ± SD of three independent experiments. ###$p < 0.001$ indicates a significance difference of normal control group from insulin resistance group. *$P < 0.05$, **$P < 0.01$, and ***$P < 0.001$ indicate significant difference of oligonol treated group from the insulin resistance group. Those results suggested oligonol attenuated glucose uptake dysfunction in insulin-resistant HepG2 cells. PTP1B, a non-transmembrane protein tyrosine phosphatase, is likely to be involved in the pathways leading to insulin resistance as a major negative regulator of insulin signaling (Panzhinskiy et al. 2013; Tiganis 2013). Furthermore, we investigate the effects of oligonol on PTP1B expression level in insulin resistance HepG2 cells, for co-relation with our previous studies. Our result showed that dose-dependently oligonol at different concentration inhibits the PTP1B expression level. Compare to the normal control and metformin group, the inhibitory activity of oligonol was higher (Fig. 17). In

the present study, we also investigated the activity, confirmation and interaction, and binding energies of the selected constituents of oligonol using docking experiments. Molecular docking simulation is a powerful and increasingly substantial tool for drug discovery (Meng et al. 2011; Morris and Lim-Wilby 2008) and can be used to screen and identify prospective biological active molecules from natural product databases (Ma et al. 2011). Using this approach, we obtained docking scores to evaluate the strength of the different protein-ligand complex interactions. Molecular docking results were obtained using Autodock 4.2 software and identify the several hydrogen bond interacting residues that were involved in PTP1B inhibition. Oligonol constituents (catechin) bound with PTP1B by forming 6 hydrogen bonds that involved the formation of three hydrogen bonds with the SER80 residue, interacting oxygen and nitrogen atom group with the hydroxyl group of catechin and had binding energies of –8.24 kcal/mol (Table 5). However, the epicatechin did share common hydrogen bond interaction with the GLY209, HIS208, SER80, LYS73 residues with catechin, and had binding energies of –8.27kcal/mol respectively. Epigallocatechin and epigallocatechin gallate formed 5, and 6 hydrogen bond respectively with binding energies -7.85 and -6.91 kcal/mol. A total of eight hydrogen bonds were observed

between procyanidin A1, and A2 with the residues ASP137 forming three, ILE134 forms two, and LYS131, GLN127 with LYS128 forming one hydrogen bonds by interacting with the hydroxyl group procyanidin A1. The binding affinity of procyanidin A1 and A2 with PTP1B was –6.85, and -8.38 kcal/mol, respectively (Table 5). Procyanidin B1 formed 5 hydrogen bond interactions with LYS73, SER80, GLN102, and LEU204 residues and had a binding affinity of –6.56 kcal/mol for PTP1B. A total of five hydrogen bonds were observed between procyanidin B2 and the residues SER80 forming two, GLU207, VAL211, and SER203 forming one hydrogen bonds by interacting with the hydroxyl group procyanidin B2. The binding affinity of procyanidin B2 with PTP1B was –7.27 kcal/mol. interestingly, identified specific interacting residues (SER80), which shared among all of the oligonol constituents except procyanidin A1, and A2, involved in PTP1B inhibition. Moreover, the several hydrophobic residues were found to strengthen the interactions between PTP1B and oligonol constituents through Vander Waals interactions. Importantly, the docking scores and binding interactions of the constituents of oligonol were significantly associated with their ability to inhibit the activity of PTP1B. Furthermore, the inhibition of PTP1B expression leads to the activation of IR as well tyrosine

phosphorylation of IRS (White 1998; White 2002), that phosphorylated IRS activates PI3K (Cross et al. 1995; Franke et al. 2003), and subsequently, the activated PI3K phosphorylates Ser/Thr kinase Akt. On the one hand, the activation of Akt promotes the translocation of intracellular GLUT4 to the plasma membrane, resulting in enhanced glucose uptake. We also investigated the effects of oligonol on the phosphorylation level of IRS-1, Akt, and PI3K of insulin signaling protein kinase. Oligonol increase the phosphorylation level of IRS-1, Akt, and PI3K at dose dependent manner that stimulates the insulin signaling. Recent studies have reported that PTP1B inhibitor increased the tyrosine phosphorylation of IR, and activated the downstream molecules of insulin signaling such as IRS-1, Akt, and ERK1 (Maeda et al. 2014; Takada et al. 2012). Additionally, oligonol stimulated the phosphorylation of ERK1 in insulin resistant HepG2 cells, a subfamily of mitogen-activated protein kinases, is a downstream kinase of insulin signaling pathway. On the other hand, inflammation is a key factor that related to the development of insulin resistance, by increased expression of inflammatory cytokines such as tumor necrosis factor alpha (TNF-α), interleukin (IL)-1 and IL-6. Inflammatory cytokines stimulate I-kappa-B (IκB) kinase-β (IKKβ) for the activation of nuclear factor-kappa B (NF-κB). After

activation, NF-κB, which translocates to the nucleus, leading to the expression of proteins inhibiting insulin signaling, this helps to the development of insulin resistance (King 2008; Hirabara et al. 2012). We also investigated the inhibitory activity of oligonol on NF-κB activation, which demonstrates that oligonol inhibits significantly NF-κB activation in insulin resistance HepG2 cells. Interestingly oligonol at concentration 5, and 10 μg/mL inhibited NF-κB more than the Metformin. Recent studies have been reported that insulin resistance is also responsible for the cell death through the caspase-3 activation. We determined the inhibitory effects of oligonol on caspase-3 activation. Caspase-3 is a caspase protein that interacts with caspase-8 and caspase-9, which plays a central role in the execution-phase of cell apoptosis in insulin resistance condition. The inhibition of caspase-3 promotes the cell survivability. At concentration 10 μg/mL, oligonol inhibit the caspase-3 protein expression as like as normal control group.

Furthermore, we investigate the effects of oligonol aginst oxidative stress that are related to the T2DM and hepatotoxicity. We hence investigated the in vitro $ONOO^-$ and total ROS scavenging activity of oligonol with the determination of *t*-BHP induced ROS generation in HepG2 cell. Among cellular oxidative stress,

ROS and RNS, including superoxide anion radical ($\cdot O_2^-$), hydrogen peroxide (H_2O_2), hydroxyl radical ($\cdot OH$), singlet oxygen (O_2), alkoxyl radical ($RO\cdot$), peroxyl radical ($ROO\cdot$), and $ONOO^-$ are responsible for liver diseases. In our study, oligonol proved to be a potent ROS inhibitor, compared to the positive control drug trolox, as well as a significant $ONOO^-$ inhibitor, compared to penicillamine. The effect of oligonol on t-BHP induced ROS generation in HepG2 cell was also significant. Enhanced ROS production is major parts of the mechanism involved in *t*-BHPinduced cytotoxicity. Both ROS and reactive nitrogen species (RNS) are known to play a central role in liver diseases such as hepatocellular carcinoma, viral and alcoholic hepatitis, and nonalcoholic steatosis. Therefore, the use of antioxidants has been suggested to prevent or alleviate the pathology of liver diseases caused by oxidative stress. Phenolic compounds, in particular polyphenols, are believed to be at least in part responsible for these effects by chelating metal ions, preventing radical formation, indirectly modulating enzyme activity and altering the expression levels of antioxidant and detoxifying enzymes (Bullo et al. 2003; Vitaglione et al. 2004; Ross and Kasum 2002). Consistent with the in-vitro assay data presented here, pretreatment of oligonol significantly attenuated the cytotoxic effect of t-

BHP at a dosage (5, and 10 μg/mL). These results indicate that the hepatoprotective properties of oligonol attributed to the direct antioxidative activity of oligonol via the scavenging of $ONOO^-$ and total ROS in the hepatocyte.

Overall, these data revealed that oligonol decreased PTP1B expression by binding to a specific site, leading to the increased phosphorylation of IRS, PI3K, Akt and ERK1 in insulin-resistant HepG2 cells, which enhance the insulin sensitivity. Oligonol also appears to exert its hepatoprotective effects by scavenging $ONOO^-$ and decreasing total as well as intracellular ROS production, thereby preventing hepatic damage. These findings suggest that oligonol is a potential regulator of PTP1B, and also is a promising anti-diabetic compound that will be helpful for the treatment of T2DM as well as may be an effective hepatoprotective agent, and could potentially be useful for preventive therapies against oxidative stress-related hepatotoxicity.

IV. Summary

Oligonol is a phenolic product, which is derived from lychee fruit, is a relatively low-molecular-weight polyphenol containing catechin-type monomers and oligomers of proanthocyanidin. Oligonol is produced by oligomerization of polyphenol polymers, typically proanthocyanidins. According to our *in vitro* enzymatic studies oligonol showed potent inhibitory activities against α-glucosidase, protein tyrosine phosphatase 1B, cholinesterase, and β-secretase 1, which are related to diabetes and Alzheimer's disease. Furthermore, HepG2 cells were used to find out the possible mechanism of oligonol against DM, and hepatoprotective activity was also examined. While, the binding mode of the particular constituents of oligonol against PTP1B was known by the molecular docking simulation. According to our results, oligonol promotes glucose uptake and protects hepatocyte by modulating the insulin signaling pathway in insulin-resistant HepG2 cells *via* PTP1B Inhibition (Fig. 30). Overall, this study suggests that oligonol has strong antidiabetic, hepatoprotective, as well as anti-Alzheimer's disease properties.

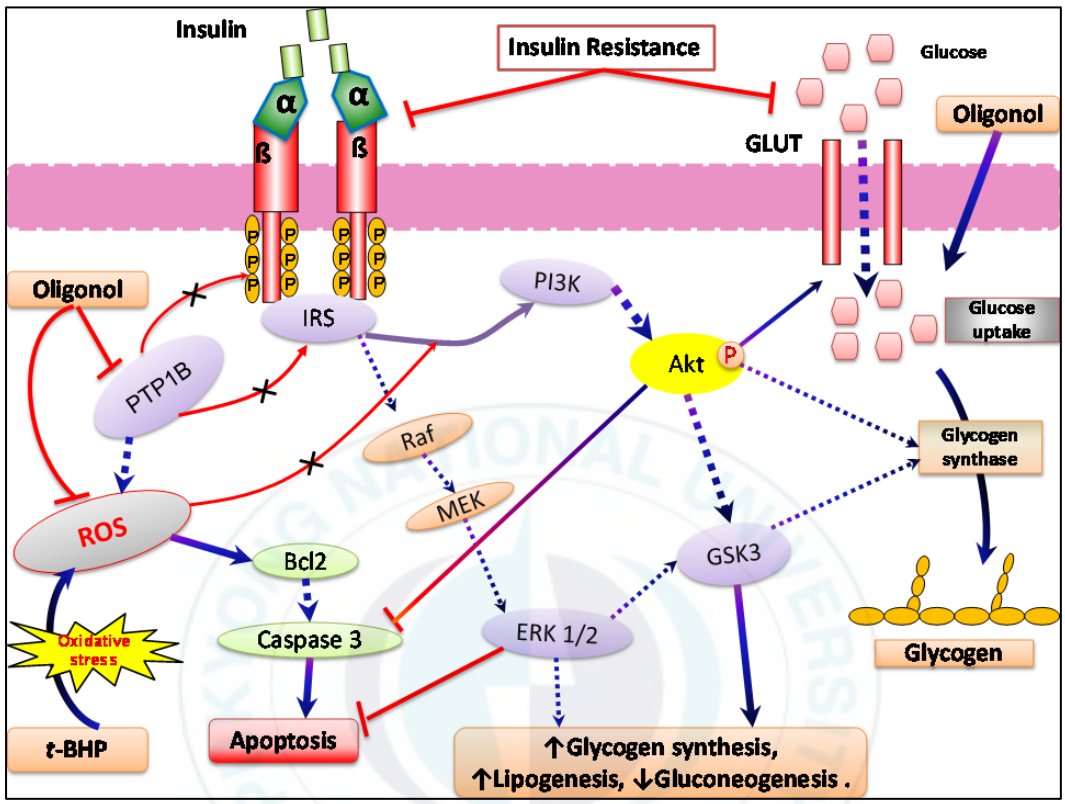

Fig. 30. Effects of oligonol on insulin resistance and possible mechanism *in vitro*.

V. References

Ahmad F, Azevedo JL, Cortright R, Dohm GL, Goldstein BJ (1997). Alterations in skeletal muscle protein-tyrosine phosphatase activity and expression in insulin-resistant human obesity and diabetes. J Clin Invest 100: 449–458.

Alessi DR, Andjelkovic M, Caudwell B, Cron P, Morrice N, Cohen P, Hemmings BA (1996). Mechanism of activation of protein kinase B by insulin and IGF-1. EMBO J 15: 6541–6551.

Avruch J (1998). Insulin signal transduction through protein kinase cascades. Mol Cell Biochem 182: 31–48.

Ayodhya S, Kusum S, Anjali S (2110). Hypoglycemic activity of different extract of various herbal plants. Int J Res Ayurveda Pharm 1: 212-224.

Banting FG, Best CH, Collip JB, Campbell WR, Fletcher AA (1922). Pancreatic extracts in the treatment of diabetes mellitus. Can Med Assoc J 12: 141–146.

Berman HM, Battistuz T, Bhat TN, Bluhm WF, Bourne PE, Burkhardt K, Feng Z, Gilliland GL, Iype L, Jain S, Fagan P, Marvin J, Padilla D, Ravichandran V, Schneider B, Thanki N, Weissig H, Westbrook JD, Zardecki C (2002). The protein data bank. Acta Crystallogr D Biol Crystallogr 58: 899–907.

Bernstein FC, Koetzle TF, Williams GJ, Meyer EFJr, Brice MD, Rodgers JR, Kennard O, Shimanouchi T, Tasumi M (1977). The protein data bank: a computer based archival file for macromolecular structures. J Mol Biol 112: 535–542.

Brat P, George S, Bellamy A, Du Chaffaut L, Scalbert A, Mennen L, Arnault N, Amiot MJ (2006). Daily polyphenol intake in France from fruit and vegetables. J Nutr 136: 2368-2373.

Bullo M, García-Lorda P, Megias I, Salas-Salvado J (2003). Systemic inflammation, adipose tissue tumor necrosis factor, and leptin expression. Obes Res 11: 525-531.

Butterfield DA, Drake J, Pocernich C, Castegna A (2001) Evidence of oxidative damage in Alzheimer's disease brain: central role for amyloid β-peptide. Trends Mol Med 7: 548–554.

Byon JC, Kusari AB, Kusari J (1998). Protein-tyrosine phosphatase-1B acts as a negative regulator of insulin signal transduction. Mol Cell Biochem 182: 101–108.

Ceriello A, Mercuri F, Quagliaro L, Assaloni R, Motz E, Tonutti L, Taboga C (2001). Detection of nitrotyrosine in the diabetic plasma: evidence of oxidative stress. Diabetologia 34: 834-838.

Chang-Chen KJ, Mullur R, Bernal-Mizrachi E (2008). β-Cell failure as a complication of diabetes. Rev Endocr Metab Disord. 9: 329-343.

Cheung A, Kusari J, Jansen D, Bandyopadhyay D, Kusari A, Bryer-Ash M (1999). Marked impairment of protein tyrosine phosphatase 1B activity in adipose tissue of obese subjects with and without type 2 diabetes mellitus. J Lab Clin Med 134: 115–123.

Choi JS, Bhakta HK, Fujii H, Min BS, Park CH, Yokozawa T, Jung HA (2016). Inhibitory evaluation of oligonol on α-glucosidase, protein tyrosine phosphatase 1B, cholinesterase, and β-secretase 1 related to diabetes and Alzheimer's disease. Arch Pharm Res 39: 409-420.

Choi JS, Islam MN, Ali MY, Kim YM, Park HJ, Sohn HS, Jung HA (2014). The effect of C-glycosylation of luteolin on its antioxidant, anti-Alzheimer's disease, anti-diabetic, and anti-inflammatory activities. Arch Pharm Res 37: 1354-1363.

Choi YY, Maeda T, Fujii H, Yokozawa T, Kim HY, Cho EJ, Shibamoto T (2014). Oligonol improves memory and cognition under an amyloid β (25-35)-induced Alzheimer's mouse model. Nutr Res 34: 595-603.

Cornier MA, Dabelea D, Hernandez TL, Lindstrom RC, Steig AJ, Stob NR (2008). The metabolic syndrome. Endocrine reviews 29: 777-822.

Cornish-Bowden A (1974). A simple graphical method for determining the inhibition constants of mixed, uncompetitive and non-competitive inhibitors. Biochem J 137: 143-144.

Cross DA, Alessi DR, Cohen P, Andjelkovich M, Hemmings BA (1995). Inhibition of glycogen synthase kinase-3 by insulin mediated by protein kinase B. Nature 378: 785–789.

Cui L, Na M, Oh H, Bae EY, Jeong DG, Ryu SE, Kim S, Kim BY, Oh WK, Ahn JS (2006). Protein tyrosine phosphatase 1B inhibitors from *Morus* root bark. Bioorg Med Chem Lett 16: 1426-1429.

Doble BW, Woodgett JR (2003). GSK-3: tricks of the trade for a multi-tasking kinase. J Cell Sci 116: 1175-1186.

Elchebly M, Payette P, Michaliszyn E, Cromlish W, Collins S, Loy AL, Normandin D, Cheng A, Himms-Hagen J, Chan CC, Ramachandran C,

Gresser MJ, Tremblay ML, Kennedy BP 9 1999). Increased insulin sensitivity and obesity resistance in mice lacking the protein tyrosine phosphatase-1B gene. Science 283: 1544–1548.

Ellman GL, Courtney KD, Andres V Jr, Feather-stone RM (1961). A new and rapid colorimetric determination of acetylcholinesterase activity. Biochem Pharmacol 7: 88-95.

Evin G, Lessene G, Wilkins S (2011). BACE inhibitors as potential drugs for the treatment of Alzheimer's disease: focus on bioactivity. Recent Pat CNS Drug Discov 6: 91-106.

Franke TF, Hornik CP, Segev L, Shostak GA, Sugimoto C (2003). PI3K/Akt and apoptosis: size matters. Oncogene 22: 8983–8998.

Franke TF, Kaplan DR, Cantley LC, Toker A (1997). Direct regulation of the Akt proto-oncogene product by phosphatidylinositol-3,4- bisphosphate. Science 275: 665–668.

Fujii H, Nishioka H, Wakame K, Magnuson BA, Roberts A (2008). Acute, subchronic and genotoxicity studies conducted with oligonol, an oligomerized polyphenol formulated from lychee and green tea extracts. Food Chem Toxicol 46: 3553-3562.

Gao F, Jian L, Zafar MI, Du W, Cai Q, Shafqat RA, Lu F (2015). 4-Hydroxyisoleucine improves insulin resistance in HepG2 cells by decreasing TNF-α and regulating the expression of insulin signal transduction proteins. Mol Med Rep 12: 6555-6560.

Gasparini L, Netzer W J, Greengard P, Xu H (2002). Does insulin dysfunction play a role in Alzheimer's disease? Trends Pharmacol Sci 23: 288−93.

Gonzalez-Rodriguez A, Escribano O, Alba J, Rondinone CM, Benito M, Valverde AM (2007). Levels of protein tyrosine phosphatase 1B determine susceptibility to apoptosis in serum-deprived hepatocytes. J Cell Physiol 212: 76–88.

Goodsell DS, Morris GM. Olson AJ (1996). Automated docking of flexible ligands: applications of autodock. J Mol Recognit 9: 1–5.

Groop PH, Forsblom C, Thomas MC (2005) Mechanisms of disease: Pathway-selective insulin resistance and microvascular complications of diabetes. Nat Clin Pract Endocrinol Metab 1: 100–110.

Grunberger D, Banerjee R, Eisinger K, Oltz EM, Efros L, Caldwell M, Estevez V, Nakanishi K (1988). Preferential cytotoxicity on tumor cells by caffeic acid phenethyl ester isolated from propolis. Experientia 44: 230– 232.

Gum RJ, Gaede LL, Koterski SL, Heindel M, Clampit JE, Zinker BA, Trevillyan JM, Ulrich RG, Jirousek MR, Rondinone CM (2003). Reduction of protein tyrosine phosphatase 1B increases insulin-dependent signaling in ob/ob mice. Diabetes 52: 21–28.

Haan MN (2006). Therapy insight: type 2 diabetes mellitus and the risk of late-onset Alzheimer's disease. Nat Clin Pract Neurol 2:159-166.

Hirabara SM, Gorjao R, Vinolo MA, Rodrigues AC, Nachbar RT, Curi R (2012). Molecular targets related to inflammation and insulin resistance and potential interventions. J Biomed Biotechnol 2012: 1-16.

Hsieh TC, Wu JM (1999). Differential effects on growth, cell cycle arrest, and induction of apoptosis by resveratrol in human prostate cancer cell lines. Exp Cell Res 249: 109-115.

Jiang G, Lin S, Wen L, Jiang Y, Zhao M, Chen F, Prasad KN, Duan X, Yang B (2013). Identification of a novel phenolic compound in litchi (Litchi chinensis Sonn.) pericarp and bioactivity evaluation. Food Chem 136: 563-568.

Jo EH, Lee SJ, Ahn NS, Park JS, Hwang JW, Kim SH, Aruoma OI, Lee YS, Kang KS (2007). Induction of apoptosis in MCF-7 and MDA-MB-231

breast cancer cells by oligonol is mediated by Bcl-2 family regulation and MEK/ERK signaling. Eur J Cancer Prev 16: 342-347.

Johnson TO, Ermolieff J, Jirousek MR (2002). Protein tyrosine phosphatase 1B inhibitors for diabetes. Nat Rev Drug Discov 1: 696-709.

Jones G, Willett P, Glen RC, Leach AR, Taylor R (1997). Development and validation of a genetic algorithm for flexible docking. J Mol Biol 267: 727–748.

Jones PJ, Varady KA (2008). Are functional foods redefining nutritional requirements? Appl Physiol Nutr Metab 33: 118-123.

Jung DW, Ha HH, Zheng X, Chang YT, Williams DR (2011). Novel use of fluorescent glucose analogues to identify a new class of triazine-based insulin mimetics possessing useful secondary effects. Mol BioSyst 7: 346–358.

Jung HA, Jin SE, Choi RJ, Kim DH, Kim YS, Ryu JH, Kim DW, Son YK, Park JJ, Choi JS (2010). Anti-amnesic activity of neferine with antioxidant and anti-inflammatory capacity, as well as inhibition of ChEs and BACE1 Life Sci 87: 420-430.

Jung HA, Kim YS, Choi JS (2009). Quantitative HPLC analysis of two key flavonoids and inhibitory activities against aldose reductase from different parts of the Korean thistle, *Cirsium maackii*. Food Chem Toxicol 47: 2790-2797.

Kenner KA, Anyanwu E, Olefsky JM, Kusari J (1996). Protein-tyrosine phosphatase 1B is a negative regulator of Insulin- and Insulin-like growth factor-I-stimulated signaling. J Biol Chem 271: 19810–19816.

Kim JS, Kwon CS, Son KH (2000). Inhibition of alpha glucosidase and amylase by luteolin, a flavonoid. Biosci Biotechnol Biochem 64: 2458-2461.

King GL (2008). The role of inflammatory cytokines in diabetes and its complications. J Periodontol 79: 1527- 1534.

Kitadate K, Homma K, Roberts A, Maeda T (2014). Thirteen-week oral dose toxicity study of oligonol containing oligomerized polyphenols extracted from lychee and green tea. Regul Toxicol Pharmacol 68: 140-146.

Klaman LD, Boss O, Peroni OD, Kim JK, Martino JL, Zabolotny JM, Moghal N, Lubkin M, Kim YB, Sharpe AH (2000). Increased energy expenditure, decreased adiposity, and tissue-specific insulin sensitivity in protein-tyrosine phosphatase 1B-deficient mice. Mol Cell Biol 20: 5479–5489.

Klover PJ, Mooney RA (2004). Hepatocytes: critical for glucose homeostasis. Int J Biochem Cell Biol 36: 753–758.

Kooy NW, Royall JA, Ischiropoulos H, Beckman JS (1994). Peroxynitrite-mediated oxidation of dihydrorhodamine 123. Free Radicl Biol Med 16: 149–156.

Kundu JK, Chang EJ, Fujii H, Sun B, Surh YJ (2008). Oligonol inhibits UVB-induced COX-2 expression in HR-1 hairless mouse skin AP-1 and C/EBP as potential upstream targets. Photochem Photobiol 84: 399-406.

Kusari J, Kenner KA, Shu KI, Hill DE, Henry RR (1994). Skeletal muscle protein tyrosine phosphatase activity and tyrosine phosphatase 1B protein content are associated with insulin action and resistance. J Clin Invest 93: 1156-1162.

Kuwabara T, Kagalwala MN, Onuma Y, Ito Y, Warashina M, Terashima K, Sanosaka T, Nakashima K, Gage FH, Asashima M (2011). Insulin biosynthesis in neuronal progenitors derived from adult hippocampus and the olfactory bulb. EMBO Mol Med 3: 742–754.

Kwon SH, Lee HK, Kim JA, Hong SI, Kim HC, Jo TH, Park YI, Lee CK, Kim YB, Lee SY, Jang CG (2010). Neuroprotective effects of chlorogenic acid

on scopolamine-induced amnesia via anti-acetylcholinesterase and anti-oxidative activities in mice. Eur J Pharmacol 649: 210-217.

Lacroix MC, Badonnel K, Meunier N, Tan F, Schlegel-Le Poupon C, Durieux D, Monnerie R, Baly C, Congar P, Salesse R (2008). Expression of insulin system in the olfactory epithelium: First approaches to its role and regulation. J Neuroendocrinol 20: 1176–1190.

Lebel CP, Bondy SC (1990). Sensitive and rapid quantitation of oxygen reactive species formation in rat synaptosomes. Neurochemistry International 17: 435–440.

Li MH, Jang JH, Sun B, Surh YJ (2004). Protective effects of oligomers of grape seed polyphenols against beta-amyloid induced oxidative cell death. Ann N Y Acad Sci 1030: 317–329.

Li T, Zhzng XD, Song YW, Liu WA (2005). A microplate based screening method for α-glucosidase inhibitors. Chin J Clin Pharmacol Therape 10: 1128-1134.

Lin L (2008). Commonality between diabetes and Alzheimer's disease and a new strategy for the therapy. Clin Med Pathol 1: 83-91.

Lineweaver H, Burk D (1934). The determination of enzyme dissociation constants. J Am Chem Soc 56: 658-666.

Ling X, Martins RN, Racchi M, Craft S, Helmerhorst E (2002). Amyloid beta antagonizes insulin promoted secretion of the amyloid beta protein precursor. J Alzheimer's Dis 4: 369−374.

Liu Z-Q, Liua T, Chena C, Li M-Y, Wang Z-Y, Chen R-S, Wei G-X, Wang X-Y, Luo D-Q (2015). Fumosorinone, a novel PTP1B inhibitor, activates insulin signaling in insulin-resistance HepG2 cells and shows anti-diabetic effect in diabetic KKAy mice. Toxicol Appl Pharmacol 285: 61-70.

Luo J, Wärmländer SK, Gräslund A, Abrahams JP (2016). Reciprocal molecular interactions between the Aβ peptide linked to Alzheimer's disease and insulin linked to diabetes mellitus type II. ACS Chem Neurosci 7: 269-74.

Ma D-L, Chan DS-H, Leung C-H (2011). Molecular docking for virtual screening of natural product databases. Chem Sci 2: 1656–1665.

Maeda A, Kai K, Ishii M, Ishii T, Akagawa M (2014). Safranal, a novel protein tyrosine phosphatase 1B inhibitor, activates insulin signaling in C2C12 myotubes and improves glucose tolerance in diabetic KK-Ay mice. Mol Nutr Food Res 58: 1177-1189.

Meng XY, Zhang HX, Mezei M, Cui M (2011). Molecular Docking: A powerful approach for structure-based drug discovery. Curr Comput Aided Drug Des 7: 146–157.

Morris GM, Lim-Wilby M (2008). Molecular docking. Methods Mol Biol 443: 365–382.

Mossman T (1983). Rapid colorimetric assay for cellular growth and survival: application to proliferation and cytotoxic assays. J Immunol Methods 65: 55–63.

Mukherjee B, Hossain CM, Mondal L, Paul P, Ghosh MK (2013). Obesity and insulin resistance: an abridged molecular correlation. Lipid Insights 6: 1-11.

Nakayama M, Suzuki K, Toda M, Okubo S, Hara Y, Shimamura T (1993). Inhibition of the infectivity of influenza virus by tea polyphenols. Antiviral Res 21: 289-299.

Newgard CB, Brady MJ, O'Doherty RM, Saltiel AR (2000). Organizing glucose disposal: emerging roles of the glycogen targeting subunits of protein phosphatase-1. Diabetes 49: 1967–1977.

Nishioka H, Fujii H, Sun B, Aruoma OI (2006). Comparative efficacy of oligonol, catechin and (-)-epigallocatechin 3-O-gallate in modulating the potassium bromate-induced renal toxicity in rats. Toxicology 226: 181-187.

Noh JS, Kim HY, Park CH, Fujii H, Yokozawa T (2010). Hypolipidaemic and antioxidative effects of oligonol, a low-molecular weight polyphenol derived from lychee fruit, on renal damage in type 2 diabetic mice. Br J Nutr 104: 1120–1128.

Noh JS, Park CH, Yokozawa T (2011). Treatment with oligonol, a low-molecular polyphenol derived from lychee fruit, attenuates diabetes-induced hepatic damage through regulation of oxidative stress and lipid metabolism. Br J Nutr 106: 1013-1022.

Nonaka GI, Sun B, Yuan L, Nakagawa T, Fujii H, Surh YJ. Sulfur-containing proanthocyanidin oligomer composition and process for producing the same. International Patent Application No.; WO/2004/103988 A1.

Ogasawara J, Kitadate K, Nishioka H, Fujii H, Sakurai T, Kizaki T, Izawa T, Ishida H, Ohno H (2009). Oligonol, a new lychee fruit-derived low-molecular form of polyphenol, enhances lipolysis in primary rat adipocytes through activation of the ERK1/2 pathway. Phytother Res 23: 1626-1633.

Pal S, Choudhuri T, Chattopadhyay S, Bhattacharya A, Datta GK, Das T, Sa G (2001). Mechanisms of curcumin induced apoptosis of Ehrlich's ascites carcinoma cells. Biochem Biophys Res Commun 288: 658-665.

Panzhinskiy E, Ren J, Nair S (2013). Pharmacological inhibition of protein tyrosine phosphatase 1B: A promising strategy for the treatment of obesity and type 2 diabetes mellitus. Curr Med Chem 20: 2609–2625.

Park CH, Noh JS, Fujii H, Roh S-S, Song Y-O, Choi JS, Chung HY, Yokozawa T (2015). Oligonol, a low-molecular-weight polyphenol derived from lychee fruit, attenuates gluco-lipotoxicity-mediated renal disorder in type 2 diabetic *db/db* mice. Drug Discov Ther 9: 13-22.

Pessin JE, Saltiel AR (2000). Signaling pathways in insulin action: molecular targets of insulin resistance. J Clin Invest 106: 165-169.

Pettersen EF, Goddard TD, Huang CC, Couch GS, Greenblatt DM, Meng EC, Ferrin TE (2004). UCSF Chimera-a visualization system for exploratory research and analysis. J Comput Chem 25: 1605–1612.

Phiel CJ, Wilson CA, Lee VM, Klein PS (2003). GSK-3 a regulates production of Alzheimer's disease amyloid-beta peptides. Nature 423: 435−9.

Piaceri I, Nacmias B, Sorbi S (2013). Genetics of familial and sporadic Alzheimer's disease. Front Biosci (Elite Ed) 5: 167-177.

Popov D (2011). Novel protein tyrosine phosphatase 1B inhibitors: interaction requirements for improved intracellular efficacy in type 2 diabetes mellitus and obesity control. Biochem Biophys Res Commun 410: 377–381.

Qin N, Li CB, Jin MN, Shi LH, Duan HQ, Niu WY (2011). Synthesis and biological activity of novel tiliroside derivants. Eur J Med Chem 46: 5189–5195.

Qiu WQ, Folstein MF (2006). Insulin, insulin degrading enzyme and amyloid-beta peptide in Alzheimer's disease: review and hypothesis. Neurobiol Aging 27: 190−198.

Rao AA, Sridhar GR, Das UN (2007). Elevated butyrylcholinesterase and acetylcholinesterase may predict the development of type 2 diabetes mellitus and Alzheimer's disease. Med Hypotheses 69: 1272-1276.

Rarey M, Kramer B, Lengauer T, Klebe G (1996). A fast flexible docking method using an incremental construction algorithm. J Mol Biol 261: 470–489.

Reddy VP, Zhu X, Perry G, Smith MA (2009). Oxidative stress in diabetes and Alzheimer's disease. J Alzheimers Dis 16: 763-774.

Ristow M (2004). Neurodegenerative disorders associated with diabetes mellitus. J Mol Med 82: 510-529.

Rosales-Corral S, Tan DX, Manchester L, Reiter RJ (2015). Diabetes and Alzheimer disease, two overlapping pathologies with the same background: oxidative stress. Oxid Med Cell Longev 2015: 985845.

Ross JA, Kasum CM (2002). Dietary flavonoids: bioavailability, metabolic effects, and safety. Annu Rev Nutr 22: 19–34.

Sakurai T, Nishioka H, Fujii H, Nakano N, Kizaki T, Radak Z, Izawa T, Haga S, Ohno H (2008). Antioxidative effects of a new lychee fruit-derived polyphenol mixture, oligonol, converted into a low-molecular form in adipocytes. Biosci Biotechnol Biochem 72: 463-476.

Saltiel AR, Pessin JE (2002). Insulin signaling pathways in time and space. Trends Cell Biol 12: 65–71.

Sarbassov DD, Guertin DA, Ali SM, Sabatini DM (2005). Phosphorylation and regulation of Akt/PKB by the rictor-mTOR complex. Science 307:1098–1101.

Shen SC, Cheng FC, Wu NJ (2008). Effect of guava (Psidium guajava Linn.) leaf soluble solids on glucose metabolism in type 2 diabetic rats. Phytother Res 22: 1458–1464.

Shoelson SE, Lee J, Goldfine AB (2006). Inflammation and insulin resistance. J Clin Invest 116: 1793-1801.

Smith MA, Harris PLR, Sayre LM, Beckman JS, Perry G (1997). Widespread peroxynitrite-mediated damage in Alzheimer's disease. J Neurosci 17: 2653-2657.

Sridhar GR, Thota H, Allam AR, Babu CS, Prasad AS, Divakar Ch (2006). Alzheimer's disease and type 2 diabetes mellitus: the cholinesterase connection? Lipids Health Dis 5: 28.

Srikanthan P, Hsueh W. Preventing heart failure in patients with diabetes (2004). Med Clin North Am 88: 1237-1256.

Standl E, Schnell O (2012). Alpha-glucosidase inhibitors 2012 - cardiovascular considerations and trial evaluation. Diab Vasc Dis Res 9: 163-169.

Stull AJ, Wang ZQ, Zhang XH, Yu Y, Johnson WD, Cefalu WT (2012). Skeletal muscle protein tyrosinephosphatase 1B regulates insulin sensitivity in African Americans. Diabetes 61: 1415–1422.

Szczepankiewicz BG, Liu G, Hajduk PJ, Abad-Zapatero C, Pei Z, Xin Z, Lubben T, Trevillyan JM, Stashko MA, Ballaron SJ, Liang H, Huang F, Hutchins CW, Fesik SW, Jirousek MR (2003). Discovery of a potent, selective protein tyrosine phosphatase 1B inhibitor using a linked-fragment strategy. J Am Chem Soc 125: 4087-96.

Tahrani AA, Bailey CJ, Del Prato S, Barnett AH (2011). Management of type 2 diabetes: new and future developments in treatment. Lancet 378: 82–197.

Takeda S, Sato N, Rakugi H, Morishita R (2011). Molecular mechanisms linking diabetes mellitus and Alzheimer disease: beta-amyloid peptide, insulin signaling, and neuronal function. Mol Bio Syst 7: 1822−1827.

Taylor R (2012). Insulin resistance and type 2 diabetes. Diabetes 61: 778-779.

Tiganis T (2013). PTP1B and TCPTP–nonredundant phosphatases in insulin signaling and glucose homeostasis. FEBS J 280: 445–458.

Tomobe K, Fujii H, Sun B, Nishioka H, Aruoma OI (2007). Modulation of infection induced inflammation and locomotive deficit and longevity in senescence accelerated mice prone (SAMP8) model by the oligomerized polyphenol oligonol. Biomed Pharmacother 61: 427-434.

Tonks NK (2003). PTP1B: From the sidelines to the front lines! FEBS Lett 546: 140–148.

Trott O, Olson AJ (2010). Autodock vina: improving the speed and accuracy of docking with a new scoring function, efficient optimization and multithreading. J Comput Chem 31: 455–461.

Vanhaesebroeck B, Leevers SJ, Panayotou G, Waterfield MD (1997). Phosphoinositide 3-kinases: a conserved family of signal transducers. Trends Biochem Sci 22: 267–272.

Vitaglione P, Morisco F, Caporaso N, Fogliano V (2004). Dietary antioxidant compounds and liver health. Crit Rev Food Sci Nutr 44: 575–586

Wang L, Lou G, Ma Z, Liu X (2011). Chemical constituents with antioxidant activities from litchi (Litchi chinensis Sonn.) seeds. Food Chem 126:1081–1087

Wang Y, Xiang L, Wang C, Tang C, He X (2013). Antidiabetic and antioxidant effects and phytochemicals of mulberry fruit (*Morus alba* L.) polyphenol enhanced extract. Plos One 8: e71144.

Weiss R, Bremer AA, Lustig RH (2013). What is metabolic syndrome, and why are children getting it? Ann N Y Acad Sci 1281: 123-140.

White MF (1998). The IRS-signalling system: a network of docking proteins that mediate insulin action. Mol Cell Biochem 182: 3–11.

White MF (2003) Insulin signaling in health and disease. Science 302: 1710–1711.

White MF (2002). IRS proteins and the common path to diabetes. Am J Physiol Endocrinol Metab 283: 413–422.

White MF (2003) Insulin signaling in health and disease. Science 302: 1710–1711.

Xie W, Wang W, Su H, Xing D, Pan Y and Du L (2006). Effect of ethanolic extracts of *Ananas comosus* L. leaves on insulin sensitivity in rats and HepG2. Comp Biochem Physiol C Toxicol Pharmacol 143: 429-435.

Yang Y, Song W (2013). Molecular links between Alzheimer's disease and diabetes mellitus. Neuroscience 250: 140-150.

Ye J (2011). Challenges in drug discovery for thiazolidinedione substitute. Yao Xue Xue Bao 1: 137-142.

Younossi ZM, Gramlich T, Matteoni CA, Boparai N, McCullough AJ (2004). Nonalcoholic fatty liver disease in patients with type 2 diabetes. Clin Gastroenterol Hepatol 2: 262-265.

Zabolotny JM, Haj FG, Kim YB, Kim HJ, Shulman GI, Kim JK, Neel BG, Kahn BB (2004). Transgenic overexpression of protein-tyrosine phosphatase 1B in muscle causes insulin resistance, but overexpression with leukocyte antigen-related phosphatase does not additively impair insulin action. J Biol Chem 279: 24844–24851.

Zhang XH, Yokoo H, Nishioka H, Fujii H, Matsuda N, Hayashi T, Hattori Y (2010). Beneficial effect of the oligomerized polyphenol oligonol on high glucose induced changes in eNOS phosphorylation and dephosphorylation in endothelial cells. Br J Pharmacol 159: 928-938.

Zhao WQ, De Felice FG, Fernandez S, Chen H, Lambert MP, Quon MJ, Krafft G, Klein W L (2008). Amyloid beta oligomers induce impairment of neuronal insulin receptors. FASEB J 22: 246−60.